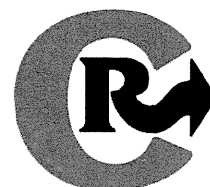




Contents lists available at ScienceDirect

Journal of Controlled Release

journal homepage: www.elsevier.com/locate/jconrel

Involvement of activated transcriptional process in efficient gene transfection using unmodified and mannose-modified bubble lipoplexes with ultrasound exposure

Keita Un ^{a,b}, Shigeru Kawakami ^{a,*}, Yuriko Higuchi ^c, Ryo Suzuki ^d, Kazuo Maruyama ^d, Fumiyoshi Yamashita ^a, Mitsuru Hashida ^{a,e,*}

^a Department of Drug Delivery Research, Graduate School of Pharmaceutical Sciences, Kyoto University, 46-29 Yoshida-Shimoadachi-cho, Sakyo-ku, Kyoto 606-8501, Japan

^b The Japan Society for the Promotion of Science (JSPS), Chiyoda-ku, Tokyo 102-8471, Japan

^c Institute for Innovative NanoBio Drug Discovery and Development, Graduate School of Pharmaceutical Sciences, Kyoto University, 46-29 Yoshida-Shimoadachi-cho, Sakyo-ku, Kyoto 606-8501, Japan

^d Department of Biopharmaceutics, School of Pharmaceutical Sciences, Teikyo University, 1091-1 Suwarashi, Midori-ku, Sagami-hara, Kanagawa 252-5195, Japan

^e Institute for Integrated Cell-Material Sciences (iCeMS), Kyoto University, Yoshida-Ushinomiya-cho, Sakyo-ku, Kyoto 606-8302, Japan

ARTICLE INFO

Article history:

Received 6 May 2011

Accepted 27 June 2011

Available online 3 July 2011

Keywords:

Gene transfection

Bubble lipoplex

Ultrasound

Transcription factor

Inflammatory response

ABSTRACT

Recently, our group developed ultrasound (US)-responsive and mannose-modified gene carriers (Man-PEG₂₀₀₀ bubble lipoplexes), and successfully obtained a high level of gene expression in mannose receptor-expressing cells following gene transfection using Man-PEG₂₀₀₀ bubble lipoplexes and US exposure. We also reported that large amounts of plasmid DNA (pDNA) were transferred into the cytoplasm of the targeted cells in the gene transfection using this method. In the present study, we investigated the involvement of transcriptional processes on enhanced gene expression obtained by unmodified and Man-PEG₂₀₀₀ bubble lipoplexes with US exposure. The transcriptional process related to activator protein-1 (AP-1) and nuclear factor-κB (NFκB) was activated by US exposure, and was found to be involved in enhanced gene expression obtained by gene transfection using unmodified and Man-PEG₂₀₀₀ bubble lipoplexes with US exposure. On the other hand, activation of AP-1 and NFκB pathways followed by US exposure was hardly involved in the inflammatory responses in the gene transfection using this method. These findings suggest that activation of AP-1 and NFκB followed by US exposure is involved in the enhanced gene expression using unmodified and Man-PEG₂₀₀₀ bubble lipoplexes with US exposure, and the selection of pDNAs activated by US exposure is important in this gene transfection method.

© 2011 Elsevier B.V. All rights reserved.

1. Introduction

Various obstacles are associated with *in vivo* gene transfection, including the control of *in vivo* distribution of nucleic acids, the improvement of intracellular/intranuclear transport of nucleic acids, and the activation of transcriptional/translational processes directly involved in the gene expression [1,2]. Viral and non-viral carriers have been studied as valuable gene carriers for *in vivo* gene transfection [3–6], with both possessing advantages and disadvantages relating to safety, productivity and gene expressing efficiency. Hama and Harashima et al. have reported that the high gene expression efficiency in gene transfection using viral carrier is influenced by the high transcriptional and translational efficiency following intranuclear transport of pDNA [7,8]. Therefore, the transcriptional/translational processes associated with gene transfection of non-

viral carriers are potentially controlled by improved gene expression efficiency.

Gene transfection methods using physical stimulation, such as electroporation method [9], hydrodynamic injection [10,11], tissue pressure-mediated method [12] and sonoporation method [13], enable to obtain high-level gene expression. Gene expression has also been reported to be enhanced by intracytoplasmic transfer of pDNA as a result of using these methods [14–16]. Recently, our group developed US-responsive and/or mannose-modified gene carriers (unmodified and Man-PEG₂₀₀₀ bubble lipoplexes), and reported that high level gene expression can be selectively obtained in mannose receptor-expressing cells following intravenous administration of Man-PEG₂₀₀₀ bubble lipoplexes and US exposure, both *in vitro* and *in vivo* [17,18]. Furthermore, we have reported that large amounts of pDNA are transferred into the cytoplasm of targeted cells in the gene transfection using unmodified and Man-PEG₂₀₀₀ bubble lipoplexes with optimized US exposure under both *in vitro* and *in vivo* conditions [19].

Various types of physical stimulations, such as electric pulse, physical pressure, radiation and US exposure, can activate the transcriptional process involved in the AP-1-mediated and NFκB-

* Corresponding authors. Tel.: +81 75 753 4545; fax: +81 75 753 4575.

E-mail addresses: kawakami@pharm.kyoto-u.ac.jp (S. Kawakami), hashidam@pharm.kyoto-u.ac.jp (M. Hashida).

mediated pathways [20–26]. It has been reported that this activation of transcription followed by physical stimulation partly contributes to the high gene expression observed when using the hydrodynamics and physical pressure-mediated methods [21,22,27]. However, there are few reports that the transcriptional process is activated by US exposure *in vivo*. Moreover, there is little information that the transcriptional activation followed by US exposure involves in the enhanced gene expression *in vitro* and *in vivo* gene transfection using sonoporation method.

Our present study investigated the involvement of transcriptional processes in enhanced gene expression obtained by transfection using unmodified and Man-PEG₂₀₀₀ bubble lipoplexes with US exposure. We examined the gene transfection efficiency obtained by US-mediated gene transfection using pDNAs controlled by various transcription factors including AP-1, NFκB, cyclic adenosine 3',5'-monophosphate response element (CRE) and serum response element (SRE), in RAW264.7 cell lines, primary mouse cultured macrophages, and mice. Then, we evaluated the gene expression and intranuclear transport of transcription factors, such as AP-1 [28] and NFκB [29,30], followed by gene transfection using unmodified and Man-PEG₂₀₀₀ bubble lipoplexes with US exposure, both *in vitro* and *in vivo*. Finally, the involvement of activated transcription on inflammatory cytokine production was also examined, since activation of specific transcriptional factors might contribute to the inflammatory responses [31,32].

2. Materials and methods

2.1. Materials

1,2-Distearoyl-*sn*-glycero-3-trimethylammoniumpropane (DSTAP), 1,2-distearoyl-*sn*-glycero-3-phosphocholine (DSPC) and 1,2-distearoyl-*sn*-glycero-3-phosphoethanolamine-N-[amino (polyethylene glycol)-2000] (NH₂-PEG₂₀₀₀-DSPE) were purchased from Avanti Polar Lipids (Alabaster, AL, USA), Sigma-Aldrich (St. Louis, MO, USA) and NOF (Tokyo, Japan), respectively. RPMI-1640 was purchased from Nissui Pharmaceutical (Tokyo, Japan) and fetal bovine serum (FBS) was purchased from Japan Bioserum (Hiroshima, Japan). All other chemicals were of the highest purity available.

2.2. pDNA, cell lines and mice

pCMV-Luc was constructed as described previously [33]. Briefly, the HindIII/Xba I firefly luciferase cDNA fragment from pGL3-control vector (Promega, Madison, WI, USA) was sub-cloned into the polylinker of pCDNA3 vector (Invitrogen, Carlsbad, CA, USA). Pathway profiling luciferase systems (pTA/Luc, pAP-1/Luc, pNFκB/Luc, pCRE/Luc and pSRE/Luc) were purchased from Clontech Laboratories (Mountain View, CA, USA). pDNA was amplified in the *Escherichia coli* strain DH5α, isolated and purified using a QIAGEN Endofree Plasmid Giga Kit (QIAGEN, Hilden, Germany). RAW264.7 cells, from a murine macrophage-like cell line, were cultured in RPMI-1640 supplemented with 10% FBS, 100 IU/ml penicillin, 100 μg/ml streptomycin, and 2 mM L-glutamine. Cells were plated onto 24-well culture plates at a density of 5×10^4 cells/1.88 cm² at 37 °C in 5% CO₂, and incubated for 48 h prior to experiments. Female ICR mice (4-week-old) and female C57BL/6 mice (6-week-old) were purchased from Japan SLC (Shizuoka, Japan). All animal experiments were carried out in accordance with the Principles of Laboratory Animal Care, as adopted and propagated by the U.S. National Institutes of Health and the Kyoto University Guidelines for Animal Experiments.

2.3. Construction of Man-PEG₂₀₀₀ bubble lipoplexes

Man-PEG₂₀₀₀ bubble lipoplexes were constructed according to our previous report [17]. Briefly, DSTAP, DSPC, and NH₂-PEG₂₀₀₀-DSPE or

mannose-modified PEG₂₀₀₀-DSPE were mixed in chloroform at a molar ratio of 7:2:1 to produce the liposomes for bubble lipoplexes. The liposome construction mixture was dried by evaporation and vacuum desiccated before the resultant lipid film was resuspended in sterile 5% dextrose. After hydration for 30 min at 65 °C, the dispersion was sonicated for 10 min in a bath sonicator and 3 min in a tip sonicator for liposome production. Liposomes were then sterilized by passage through a 0.45 μm filter (PALL, East Hills, NY, USA). Lipoplexes were prepared by gently mixing with equal volumes of pDNA and liposome solution at a charge ratio of 1.0:2.3 (–:–). Prepared lipoplexes were pressurized with perfluoropropane gas (Takachiho Chemical Industries, Tokyo, Japan) and sonicated using a bath-type sonicator (AS ONE, Osaka, Japan) for 5 min to enclose US imaging gas. Particle sizes and ζ-potentials of the liposomes/lipoplexes were determined using a Zetasizer Nano ZS instrument (Malvern Instrument, Worcestershire, UK).

2.4. Harvesting of mouse peritoneal macrophages

Mouse peritoneal macrophages were harvested and cultured as previously described [34]. Briefly, the macrophages were harvested from the peritoneal cavity of female ICR mice, before being washed and suspended in RPMI-1640 medium supplemented with 10% FBS, 100 IU/ml penicillin, 100 μg/ml streptomycin and 2 mM L-glutamine, and plated onto 24-well culture plates at a density of 2×10^5 cells/1.88 cm². After incubation for 2 h at 37 °C in 5% CO₂, non-adherent cells were washed off with culture medium, and the macrophages were incubated for another 72 h.

2.5. *In vitro* gene transfection

After RAW264.7 cells and macrophages were plated and incubated for 48 and 72 h, respectively, the culture medium was replaced with Opti-MEM I containing bubble lipoplexes (5 μg pDNA). Cells were exposed to US (frequency, 2.062 MHz; duty, 50%; burst rate, 10 Hz; intensity 4.0 W/cm²) for 20 s using a Sonopore-4000 sonicator (NEPA GENE, Chiba, Japan) with a 6 mm diameter probe placed in each well at predetermined times after the addition of bubble lipoplexes. At 1 h after addition of bubble lipoplexes, the incubation medium was replaced with RPMI-1640 and incubated for an additional time. Subsequently, the cells were scraped from the plates and suspended in lysis buffer (0.05% Triton X-100, 2 mM EDTA, 0.1 M Tris, pH 7.8). The cell suspension was shaken, and centrifuged at 10,000 × g, 4 °C for 10 min. Luciferase assay buffer (Picagene; Toyo Ink, Tokyo, Japan) was mixed with the supernatant and the luciferase activity was measured in a luminometer (Lumat LB 9507; EG&G Berthold, Bad Wildbad, Germany). Luciferase activity was normalized against the cellular protein content. Protein concentration was determined with a Protein Quantification Kit (Dojindo Molecular Technologies, Tokyo, Japan).

2.6. *In vivo* gene transfection

Mice were intravenously injected with 400 μl of bubble lipoplexes via the tail vein using a 26-gauge syringe needle at a dose of 50 μg pDNA. At predetermined times after the injection, US (frequency, 1.045 MHz; duty, 50%; burst rate, 10 Hz; intensity 1.0 W/cm²; time, 2 min) was exposed transdermally to the abdominal area using a Sonopore-4000 sonicator (NEPA GENE) with a 20 mm diameter probe. At predetermined times after injection, mice were sacrificed and organs were collected for each experiment. Organs were washed twice with cold saline and homogenized with lysis buffer (0.05% Triton X-100, 2 mM EDTA, 0.1 M Tris, pH 7.8). Lysis buffer was added at a weight ratio of 5 ml/g for the liver or 4 ml/g for other organs. After 3 cycles of freezing and thawing, the homogenates were centrifuged at 10,000 × g at 4 °C for 10 min. Luciferase activity of the resulting supernatant was determined by above-mentioned luciferase assay.

2.7. Quantitative reverse transcription-polymerase chain reaction (RT-PCR)

Total ribonucleic acid (RNA) was isolated from the cells and organs using a GenElute Mammalian Total RNA Miniprep Kit (Sigma-Aldrich). Reverse transcription of messenger RNA (mRNA) was carried out using PrimeScript[®] RT reagent Kit (Takara Bio, Shiga, Japan). The detection of complementary deoxyribonucleic acid (cDNA) (*c-fos*, *c-jun*, *p105*, *p65* and *gapdh*) was conducted using real-time PCR using SYBR[®] Premix Ex Taq (Takara Bio) and a Lightcycler Quick System 350S (Roche Diagnostics, Indianapolis, IN, USA). Primers for *c-fos*, *c-jun*, *p105*, *p65* and *gapdh* cDNA were synthesized by Sigma-Aldrich as follows: *c-fos*, 5'-CCA GTC AAG AGC ATC AGC AA-3' (forward) and 5'-AAG TAG TGC AGC CCG GAG TA-3' (reverse); *c-jun*, 5'-TCC CCT ATC GAC ATG GAG TC-3' (forward) and 5'-TGA GTT GGC ACC CAC TGT TA-3' (reverse); *p105*, 5'-CCT GGA TGA CTC TTG GGA AA-3' (forward) and 5'-TCA GCC AGC TGT TTC ATG TC-3' (reverse); *p65*, 5'-TAG CAC CTG ATG GCT GAC TG-3' (forward) and 5'-CGT TCC ACC ACA TCT GTG TC-3' (reverse); *gapdh*, 5'-TCT CCT GCG ACT TCA ACA-3' (forward) and 5'-GCT GTA GCC GTA TTC ATT GT-3' (reverse). mRNA copy number was calculated for each sample from the standard curve using the thermal-cycler software ('Arithmetic Fit Point analysis' for the Lightcycler). Results were expressed as relative copy number calculated relative to *gapdh* mRNA (*c-fos*, *c-jun*, *p105*, *p65* mRNA copy number/*gapdh* mRNA copy number).

2.8. Measurement of the level of intranuclear protein

Cells and tissues were collected at predetermined times after gene transfection, and the nuclear extract from cells and tissues was prepared using a Nuclear Extract Kit (Active Motif, Carlsbad, CA, USA). Nuclear protein was divided into aliquots and stored at -80°C for later use. The protein concentration was measured with a Protein Quantification Kit. The amounts of p50 and p65, which are the components of NF κ B in the cellular nuclear extract was measured using a NF κ B (p50) Transcription Factor Kit (Thermo Fisher Scientific, Waltham, MA, USA) and a NF κ B (p65) transcription Factor Assay Kit

(Cayman Chemical, Ann Arbor, MI, USA), respectively, according to the manufacturer's protocols.

2.9. Measurement of inflammatory cytokines

At predetermined times after the in vitro and in vivo gene transfection, the supernatants and serum were collected and the cytokine levels (TNF- α , IFN- γ , and IL-6) were determined with a commercial enzyme-linked immunosorbent assay (ELISA) Kit (Bay Bioscience, Hyogo, Japan) according to the recommended procedures.

2.10. Statistical analysis

Results were presented as the mean \pm S.D. of more than three experiments. Analysis of variance (ANOVA) was used to test the statistical significance of differences among groups. Two-group comparisons were performed by Student's *t*-test. Multiple comparisons between control and test groups were performed by Dunnett's test and multiple comparisons between all groups were performed using the Tukey–Kramer test.

3. Results

3.1. Physicochemical properties of lipoplexes and bubble lipoplexes used in this study

The physicochemical properties of lipoplexes and bubble lipoplexes constructed with various pDNAs used in all experiments were evaluated by measuring the particle sizes and ζ -potentials. Mean particle sizes and ζ -potentials of unmodified and Man-PEG₂₀₀₀ lipoplexes were approximately 137 nm and +48 mV, respectively (Supplementary Table 1). Moreover, mean particle sizes and ζ -potentials of unmodified and Man-PEG₂₀₀₀ bubble lipoplexes were approximately 550 nm and +48 mV, respectively (Supplementary Table 1). These results correspond to previous reports [17–19], suggesting that these pDNA had no effect on the physicochemical properties of lipoplexes and bubble lipoplexes.

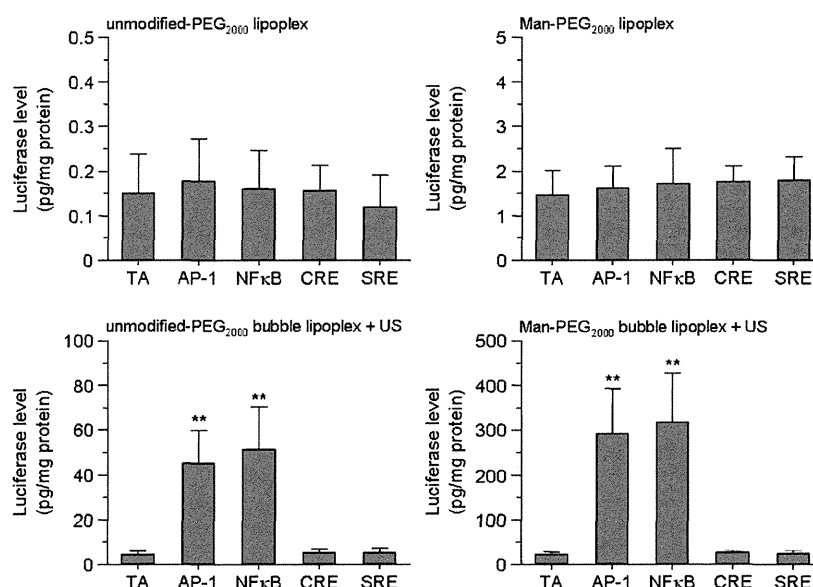


Fig. 1. The effect of transcriptional factors on gene expression obtained by unmodified and Man-PEG₂₀₀₀ bubble lipoplexes with or without US exposure in mouse cultured macrophages. Luciferase expression levels obtained by unmodified-PEG₂₀₀₀ lipoplexes, Man-PEG₂₀₀₀ lipoplexes, unmodified-PEG₂₀₀₀ bubble lipoplexes with US exposure, and Man-PEG₂₀₀₀ bubble lipoplexes with US exposure (5 μ g of pDNA) at 24 h after transfection in mouse primary cultured macrophages. Lipoplexes were constructed with pDNAs controlled by various transcription factors. Each value represents the mean \pm S.D. ($n=4$). Key: TA; pTA/Luc, AP-1; pAP-1/Luc, NF κ B; pNF κ B/Luc, CRE; pCRE/Luc, SRE; pSRE/Luc. ** $p<0.01$, compared with the corresponding TA group.

3.2. Involvement of transcriptional process on enhanced gene expression obtained by unmodified and Man-PEG₂₀₀₀ bubble lipoplexes with US exposure in vitro

The involvement of transcription on enhanced gene expression obtained by unmodified and Man-PEG₂₀₀₀ bubble lipoplexes with US exposure was investigated in mouse primary cultured macrophages. First, we examined gene expression levels using unmodified/Man-PEG₂₀₀₀ lipoplexes or bubble lipoplexes constructed with luciferase expressing-pDNA controlled by various transcription factors, including AP-1, NFκB, CRE and SRE. Gene expression levels obtained by Man-PEG₂₀₀₀ lipoplexes only or Man-PEG₂₀₀₀ bubble lipoplexes with US exposure were higher than those by unmodified-PEG₂₀₀₀ formulations (Fig. 1), since mouse cultured macrophages express the mannose receptors abundantly. Moreover, although the level of gene expression

obtained by both lipoplexes was similar in all pDNAs, the level of gene expression obtained by both bubble lipoplexes and US exposure was enhanced approximately 10-fold by gene transfection using pAP-1/Luc and pNFκB/Luc, compared with that using pTA/Luc, which is a pDNA without transcription factor-binding site within the enhancer region (Fig. 1). Similar results were observed in the murine macrophage-like RAW264.7 cells (Supplementary Fig. 1).

3.3. Involvement of transcriptional process on enhanced gene expression obtained by unmodified and Man-PEG₂₀₀₀ bubble lipoplexes with US exposure in mice

Next, we investigated the level of gene expression by in vivo gene transfection using unmodified/Man-PEG₂₀₀₀ lipoplexes and bubble lipoplexes constructed with luciferase expressing-pDNA controlled by

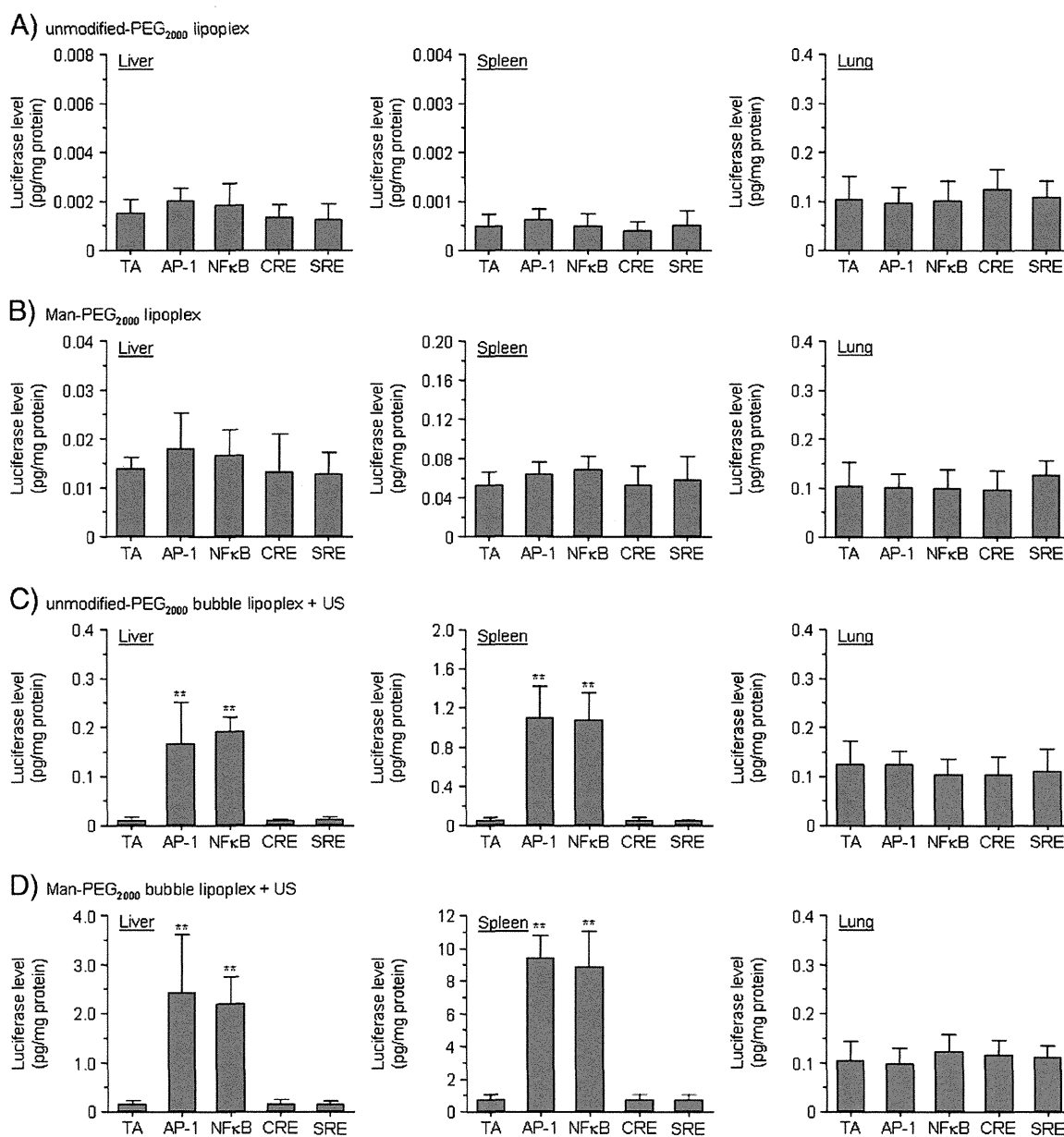


Fig. 2. The effect of transcriptional factors on gene expression obtained by unmodified and Man-PEG₂₀₀₀ bubble lipoplexes with or without US exposure in vivo. Luciferase expression levels obtained by unmodified-PEG₂₀₀₀ lipoplexes (A), Man-PEG₂₀₀₀ lipoplexes (B), unmodified-PEG₂₀₀₀ bubble lipoplexes with US exposure (C), and Man-PEG₂₀₀₀ bubble lipoplexes with US exposure (D) (50 μg of pDNA) in the liver, spleen and lung at 6 h after transfection. Lipoplexes were constructed with pDNAs controlled by various types of transcriptional factors. Each value represents the mean + S.D. (n = 4). Key: TA; pTA/Luc, AP-1; pAP-1/Luc, NFκB; pNFκB/Luc, CRE; pCRE/Luc, SRE; pSRE/Luc. **p < 0.01, compared with the corresponding TA group.

various transcription factors. Gene expression levels in the liver and spleen obtained by Man-PEG₂₀₀₀ lipoplexes only or Man-PEG₂₀₀₀ bubble lipoplexes with US exposure were higher than those by unmodified-PEG₂₀₀₀ formulations (Fig. 2), since liver and spleen are the major target organ of mannose-modified carriers. Although the level of gene expression obtained by both lipoplexes was similar in all pDNAs (Fig. 2A and B), gene expression levels in the liver and spleen obtained by both bubble lipoplexes and US exposure were enhanced approximately 10-fold by gene transfection using pAP-1/Luc and pNFκB/Luc, compared with that using pTA/Luc (Fig. 2C and D). On the other hand, enhanced gene expression followed by gene transfection using bubble lipoplexes constructed with pAP-1/Luc or pNFκB/Luc was not observed in the lung.

3.4. The effect of *in vitro* gene transfection using unmodified and Man-PEG₂₀₀₀ bubble lipoplexes with US exposure on AP-1 and NFκB

Following examination of the expression properties for *c-fos* and *c-jun*, which are the components of AP-1, *c-fos* and *c-jun* mRNA expression was enhanced transiently in mouse primary cultured macrophages by not only the gene transfection using bubble lipoplexes and US exposure, but also US exposure alone (Fig. 3A). Moreover, enhanced expression of *c-fos* and *c-jun* mRNA was not observed in the gene transfection using lipoplexes only (Fig. 3A). Evaluation of the expressing properties and intranuclear transporting properties of NFκB followed by gene transfection revealed that *p105* (precursor of p50) and *p65* mRNA expression in mouse primary cultured macrophages was not enhanced in all of groups, which differed from the results obtained for *c-fos* and *c-jun* mRNA (Supplementary Fig. 2). In contrast, the amount of intranuclear p50 and p65 increased transiently by not only the gene transfection using bubble lipoplexes and US exposure, but also US exposure alone (Fig. 3B). On the other hand, enhanced intranuclear transport of p50 and p65 was not observed in the gene transfection using lipoplexes only (Fig. 3B). Moreover, these transient AP-1 expression and intranuclear transport of NFκB followed by US exposure were also observed in RAW264.7 cells in this gene transfection method

(Supplementary Fig. 3). These results suggest that transcription activation, such as increased AP-1 expression and enhanced intranuclear transport of NFκB, is partly involved in enhanced gene expression produced by unmodified and Man-PEG₂₀₀₀ bubble lipoplexes with US exposure.

3.5. The effect of *in vivo* gene transfection using unmodified and Man-PEG₂₀₀₀ bubble lipoplexes with US exposure on AP-1 and NFκB

c-fos/c-jun mRNA expression and the intranuclear amount of p50/p65 were enhanced transiently by not only the gene transfection using bubble lipoplexes and US exposure, but also US exposure alone in both the liver and spleen (Figs. 4 and 5). On the other hand, these phenomena were not observed in the lung (Figs. 4C and 5C). In addition, *c-fos* and *c-jun* mRNA expression levels in the liver and spleen followed by US exposure were dependent on the US intensity (Supplementary Fig. 4).

3.6. The effect of *in vitro* and *in vivo* gene transfection using unmodified and Man-PEG₂₀₀₀ bubble lipoplexes and US exposure on inflammatory cytokine production

Increased AP-1 expression and intranuclear transport of NFκB followed by US exposure were demonstrated to be involved in the enhanced gene expression by unmodified and Man-PEG₂₀₀₀ bubble lipoplexes with US exposure. On the other hand, since these phenomena are potentially involved in the production of inflammatory cytokines [31,32], the production properties of inflammatory cytokines followed by gene transfection were investigated *in vitro* and *in vivo*. Although TNF-α production followed by gene transfection using only lipoplexes was significantly increased time-dependently in RAW264.7 cells and mouse primary cultured macrophages, only a slight increase in TNF-α production was observed followed by gene transfection using bubble lipoplexes and US exposure (Fig. 6).

While the inflammatory cytokines (TNF-α, IFN-γ, and IL-6) in the serum followed by *in vivo* gene transfection exhibited transient and significant increases in all of gene transfection methods (Fig. 7), the

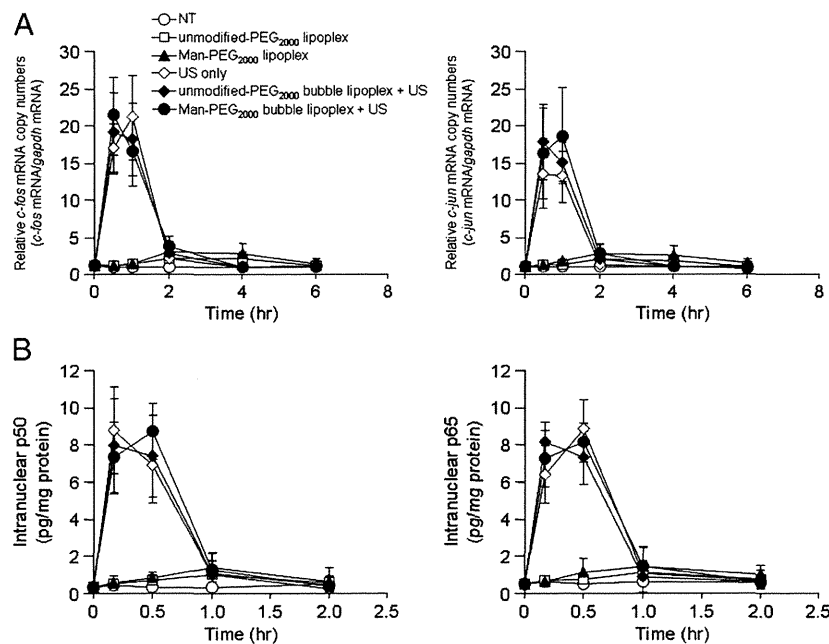


Fig. 3. Enhanced *c-fos/c-jun* mRNA expression and intranuclear transport of p105/p65 followed by gene transfection using unmodified and Man-PEG₂₀₀₀ bubble lipoplexes with or without US exposure in mouse primary cultured macrophages. Time-course of *c-fos/c-jun* mRNA expression levels (A) and intranuclear p105/p65 levels (B) followed by various transfection methods (5 μg of pCMV-Luc) in mouse primary cultured macrophages. Each value represents the mean ± S.D. (n = 4). ** p < 0.01, compared with the corresponding non-treatment (NT) group.

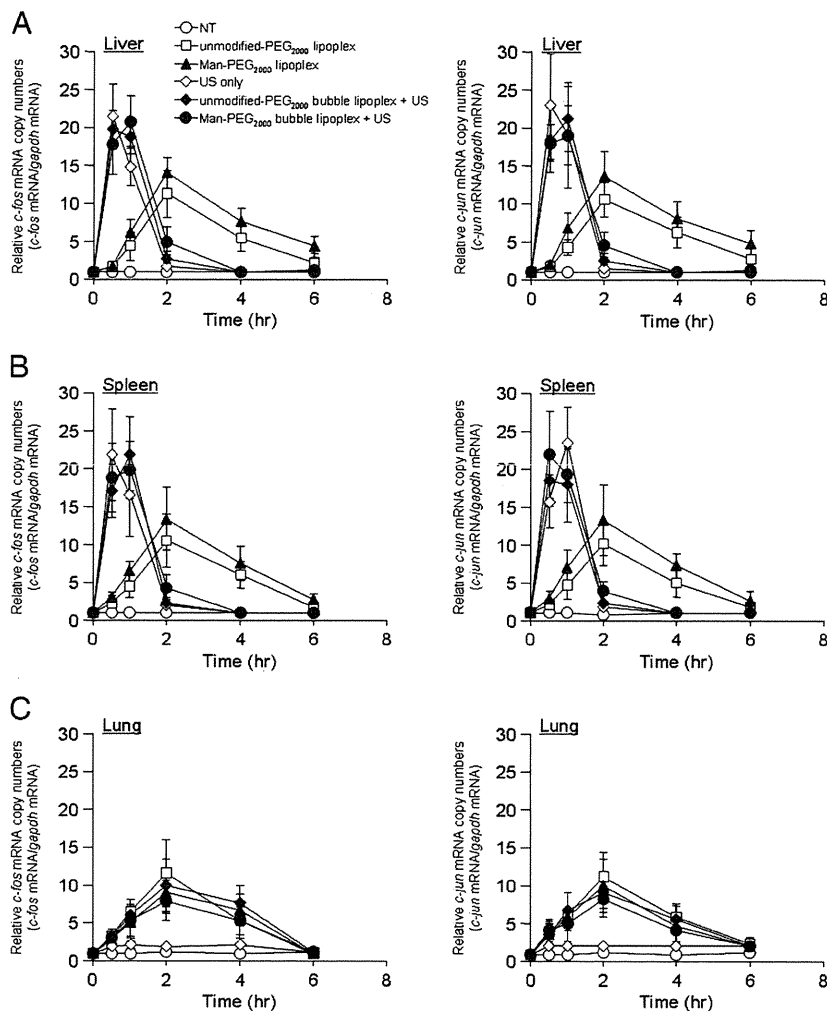


Fig. 4. Enhanced *c-fos/c-jun* mRNA expression followed by gene transfection using unmodified and Man-PEG₂₀₀₀ bubble lipoplexes with or without US exposure in vivo. Time-course of *c-fos* and *c-jun* mRNA expression levels in the liver (A), spleen (B), and lung (C) followed by various transfection methods (50 µg of pCMV-Luc) in mice. Each value represents the mean ± S.D. (n = 4). NT, non-treatment.

maximum amount of secreted inflammatory cytokines followed by gene transfection using bubble lipoplexes and US exposure was 3-fold lower than that using lipoplexes only. Moreover, the time-to-maximum concentration of secreted inflammatory cytokines followed by gene transfection using bubble lipoplexes and US exposure was earlier than that using only lipoplexes (Fig. 7). These results suggest that the production properties of inflammatory cytokine are different between conventional lipofection methods and US-mediated gene transfection methods, and that inflammatory cytokines have a minor effect on enhanced AP-1 expression/NFκB intranuclear transport followed by US exposure.

4. Discussion

We recently reported that large amounts of pDNA are directly transferred into the cytoplasm in the gene transfection using unmodified and Man-PEG₂₀₀₀ bubble lipoplexes with US exposure [17,19]. However, this enhanced gene expression followed by gene transfection using unmodified and Man-PEG₂₀₀₀ bubble lipoplexes with US exposure may not correspond to the increase of intracellular pDNA by targeted delivery of pDNA and intracytoplasmic transfer of pDNA; suggesting the involvement of the other factors on the enhanced gene expression in the gene transfection using both bubble lipoplexes and US exposure. It has

been reported that the transcriptional process following intranuclear transport of pDNA is important factor in gene transfection efficiency [7,8]; therefore, we investigated the involvement of transcriptional processes in gene transfection using unmodified and Man-PEG₂₀₀₀ bubble lipoplexes with US exposure.

Following examination of gene expression levels using luciferase-expressing pDNAs controlled by various transcription factors, including AP-1, NFκB, CRE and SRE, we found that the level of gene expression obtained by both lipoplexes in vitro (Fig. 1 and Supplementary Fig. 1), and in mouse liver and spleen (Fig. 2A and B), was similar in all pDNAs studied. On the other hand, gene expression levels using pAP-1/Luc and pNFκB/Luc were approximately 10-fold higher than those using other pDNAs in the gene transfection using unmodified and Man-PEG₂₀₀₀ bubble lipoplexes with US exposure in vitro (Fig. 1 and Supplementary Fig. 1), and in mouse liver and spleen (Fig. 2C and D). These results strongly suggest that AP-1 and NFκB were involved in the enhanced gene expression obtained by unmodified and Man-PEG₂₀₀₀ bubble lipoplexes with US exposure. Therefore, we further investigated the AP-1/NFκB gene expression and intranuclear transport followed by this gene transfection method.

c-fos/c-jun mRNA expression (Figs. 3A and 4) and intranuclear p50/p65 levels (Figs. 3B and 5) were enhanced transiently by not only the gene transfection using both bubble lipoplexes and US exposure,

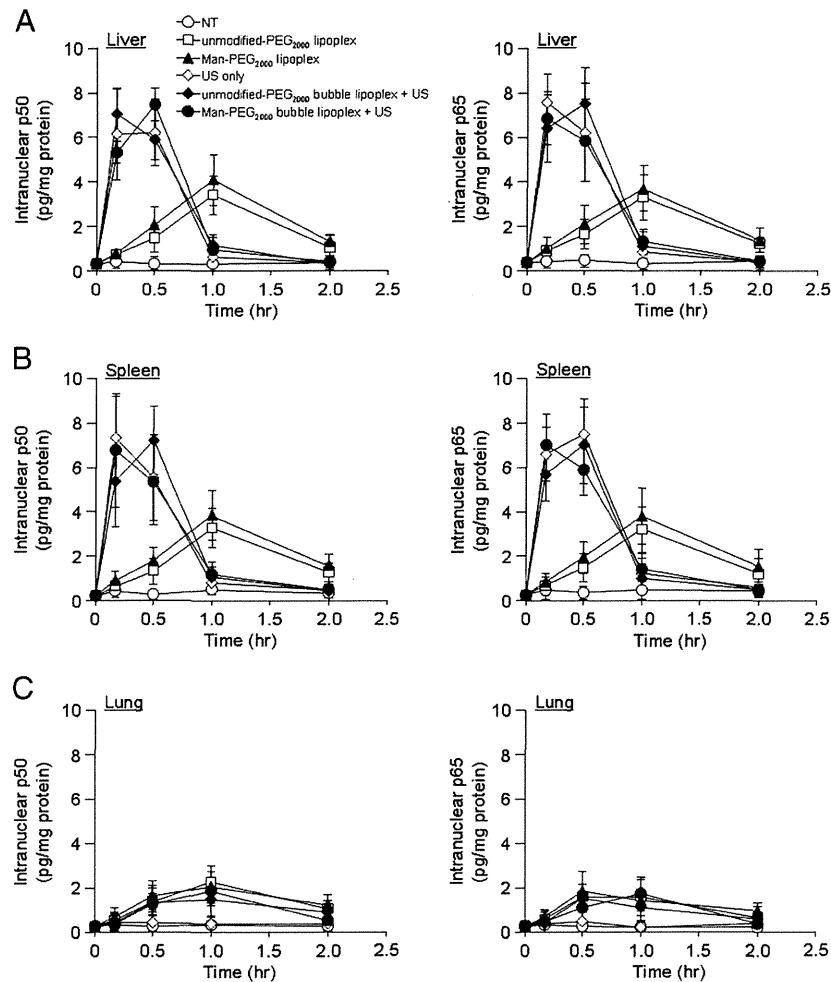


Fig. 5. Enhanced intranuclear transport of p50 and p65 followed by gene transfection using unmodified and Man-PEG₂₀₀₀ bubble lipoplexes with or without US exposure in vivo. Time-course of intranuclear p50 and p65 levels in the liver (A), spleen (B), and lung (C) followed by various transfection methods (50 μ g of pCMV-Luc) in mice. Each value represents the mean \pm S.D. ($n = 3$). NT; non-treatment.

but also US exposure alone in vitro, and in mouse liver and spleen. It has been reported that US exposure induced the enhanced expression of *c-fos* and *c-jun* via phosphorylation of ERK, p38 and JNK [25,26], and our results partially correspond to these reports. These observations led us to believe that the activation of AP-1 and NF κ B-mediated transcriptional processes followed by US exposure is involved in the enhanced gene expression using unmodified and Man-PEG₂₀₀₀ bubble lipoplexes with US exposure.

Since the activation of transcription factors such as AP-1 [28] and NF κ B [29,30] is involved in the induction of inflammatory responses [31,32], we investigated the production properties of inflammatory cytokines followed by this gene transfection method. The production levels of TNF- α , IFN- γ or IL-6 followed by gene transfection using both bubble lipoplexes and US exposure were substantially lower than that using both lipoplexes in vitro (Fig. 6) and in vivo (Fig. 7). We previously reported that the inflammatory responses were significantly suppressed in the gene transfection method using unmodified and Man-PEG₂₀₀₀ bubble lipoplexes with US exposure, because a large amount of pDNA was transferred into the cytoplasm directly through the transient pores created by the destruction of both bubble lipoplexes followed by US exposure [19], suggesting that pDNA is hardly interacted with endosomal TLR-9. On the other hand, it was reported that the phosphorylation of AP-1 and NF κ B was induced via the activation of p38, ERK and JNK-mediated pathways followed by US

exposure [25,26], and we showed that these AP-1 and NF κ B activation was transiently in our sonoporation method and condition in this study (Figs. 3–5 and Supplementary Fig. 3). Although these activation of AP-1 and NF κ B leads to the inflammatory cytokine production [31,32], the inflammatory responses induced by AP-1 and NF κ B activation followed by US exposure were low under in vitro and in vivo condition (Figs. 6 and 7). We previously have reported that the activating level of transcriptional factors, such as *c-fos* and *c-jun*, in tissue pressure-mediated transfection method was approximately one-fifth, compared with that in hydrodynamics method [22]. Moreover, the production of inflammatory cytokines under in vivo condition followed by tissue pressure-mediated transfection method was much lower than those by conventional lipofection method [35]. The activating levels of transcriptional factors followed by our sonoporation method using unmodified and Man-PEG₂₀₀₀ bubble lipoplexes with US exposure were almost the same with that by tissue pressure-mediated transfection method. Therefore, the contribution of the inflammatory response induced by AP-1 and NF κ B activation followed by our sonoporation method may be negligible. These results suggest that the transient expression of AP-1 and the transient intranuclear transport of NF κ B followed by US exposure might be minimally involved in the inflammatory responses in the gene transfection using unmodified and Man-PEG₂₀₀₀ bubble lipoplexes with US exposure.

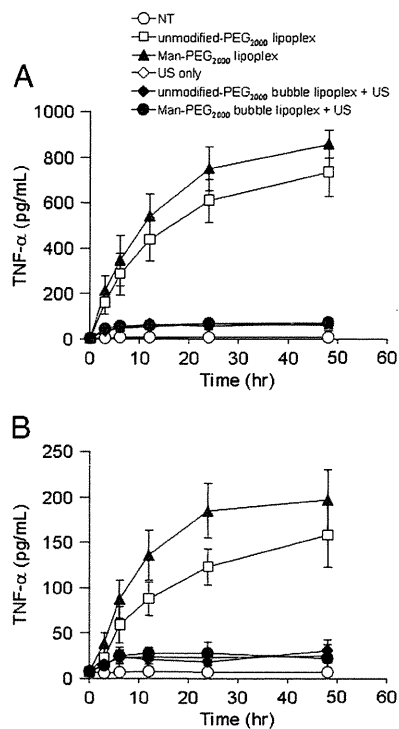


Fig. 6. Evaluation of TNF- α secretion followed by gene transfection using unmodified and Man-PEG₂₀₀₀ bubble lipoplexes with or without US exposure in vitro. TNF- α concentration in the supernatant was measured following various transfection methods (5 μ g of pDNA) at predetermined times in RAW264.7 cells (A) and mouse primary cultured macrophages (B). Each value represents the mean \pm S.D. ($n = 4$).

5. Conclusion

Our results suggest that the activated AP-1 and NF κ B followed by US exposure is involved in the enhanced gene expression using unmodified and Man-PEG₂₀₀₀ bubble lipoplexes with US exposure. These results suggest that enhanced gene expression in the gene transfection using our sonoporation method was obtained by applying pDNA controlled by the specific transcriptional factors. Therefore, the selection of suitable pDNA with specific promoter regions activated by US stimulation is one of the important factors for efficient gene expression in our gene transfection method. In addition, the transient expression of AP-1 and the transient intranuclear transport of NF κ B followed by US exposure were not substantially involved in the inflammatory responses in this gene transfection method. These findings may help in the development of an effective gene transfection method using US-exposing system.

Acknowledgments

This work was supported in part by a Grant-in-Aid for Young Scientists (A) from the Ministry of Education, Culture, Sports, Science and Technology of Japan, and by Health and Labour Sciences Research Grants for Research on Noninvasive and Minimally Invasive Medical Devices from the Ministry of Health, Labour and Welfare of Japan, and by the Programs for Promotion of Fundamental Studies in Health Sciences of the National Institute of Biomedical Innovation (NIBIO).

Appendix A. Supplementary data

Supplementary data to this article can be found online at doi:10.1016/j.jconrel.2011.06.040.

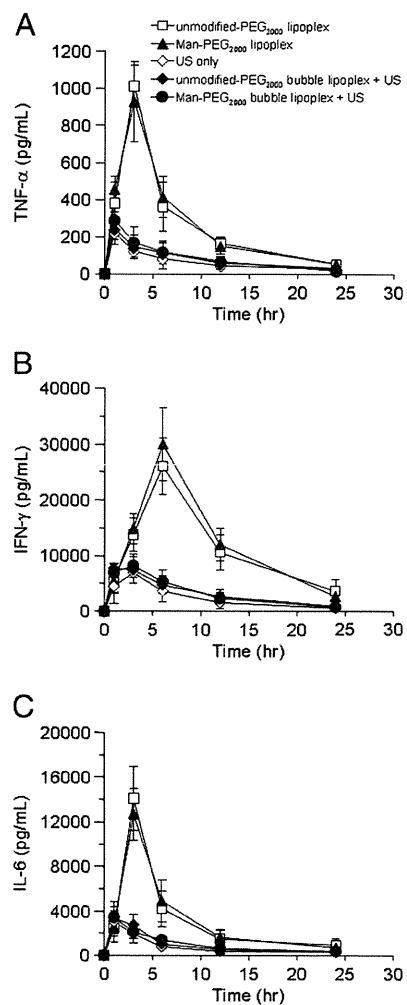


Fig. 7. Evaluation of pro-inflammatory cytokine secretion in serum followed by gene transfection using unmodified and Man-PEG₂₀₀₀ bubble lipoplexes with or without US exposure in vivo. TNF- α (A), IFN- γ (B), and IL-6 (C) concentrations in the serum were measured following various transfection methods (50 μ g of pDNA) at predetermined times in mice. Each value represents the mean \pm S.D. ($n = 4$).

References

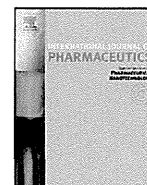
- [1] M. Thomas, A.M. Klibanov, Non-viral gene therapy: polycation-mediated DNA delivery, *Appl. Microbiol. Biotechnol.* 2003 (2003) 27–34.
- [2] T. Ito, N. Iida-Tanaka, T. Niidome, T. Kawano, K. Kubo, K. Yoshikawa, T. Sato, Z. Yang, Y. Koyama, Hyaluronic acid and its derivative as a multi-functional gene expression enhancer: protection from non-specific interactions, adhesion to targeted cells, and transcriptional activation, *J. Control. Release* 112 (2006) 382–388.
- [3] D.G. Miller, P.R. Wang, L.M. Petek, R.K. Hirata, M.S. Sands, D.W. Russell, Gene targeting in vivo by adeno-associated virus vectors, *Nat. Biotechnol.* 24 (2006) 1022–1026.
- [4] K. Itaka, K. Yamauchi, A. Harada, K. Nakamura, H. Kawaguchi, K. Kataoka, Polyion complex micelles from plasmid DNA and poly(ethylene glycol)-poly(L-lysine) block copolymer as serum-tolerable polyplex system: physicochemical properties of micelles relevant to gene transfection efficiency, *Biomaterials* 24 (2003) 4495–4506.
- [5] A. Kim, E.H. Lee, S.H. Choi, C.K. Kim, In vitro and in vivo transfection efficiency of a novel ultradeformable cationic liposome, *Biomaterials* 25 (2004) 305–313.
- [6] S.M. Kwon, H.Y. Nam, T. Nam, K. Park, S. Lee, K. Kim, I.C. Kwon, J. Kim, D. Kang, J.H. Park, S.Y. Jeong, In vivo time-dependent gene expression of cationic lipid-based emulsion as a stable and biocompatible non-viral gene carrier, *J. Control. Release* 128 (2008) 89–97.
- [7] S. Hama, H. Akita, R. Ito, H. Mizuguchi, T. Hayakawa, H. Harashima, Quantitative comparison of intracellular trafficking and nuclear transcription between adenoviral and lipoplex systems, *Mol. Ther.* 13 (2006) 786–794.
- [8] S. Hama, H. Akita, S. Iida, H. Mizuguchi, H. Harashima, Quantitative and mechanism-based investigation of post-nuclear delivery events between adenovirus and lipoplex, *Nucleic Acids Res.* 35 (2007) 1533–1543.

- [9] H. Potter, L. Weir, P. Leder, Enhancer-dependent expression of human kappa immunoglobulin genes introduced into mouse pre-B lymphocytes by electroporation, *Proc. Natl. Acad. Sci. U.S.A.* 81 (1984) 7161–7165.
- [10] F. Liu, Y. Song, D. Liu, Hydrodynamics-based transfection in animals by systemic administration of plasmid DNA, *Gene Ther.* 6 (1999) 1258–1266.
- [11] Y. He, A.A. Pimenov, J.V. Nayak, J. Plowey, L.D. Faló Jr., L. Huang, Intravenous injection of naked DNA encoding secreted flt3 ligand dramatically increases the number of dendritic cells and natural killer cells in vivo, *Hum. Gene Ther.* 11 (2000) 547–554.
- [12] F. Liu, L. Huang, Noninvasive gene delivery to the liver by mechanical massage, *Hepatology* 35 (2002) 1314–1319.
- [13] K. Anwer, G. Kao, B. Proctor, I. Anscombe, V. Florack, R. Earls, E. Wilson, T. McCreery, E. Unger, A. Rolland, S.M. Sullivan, Ultrasound enhancement of cationic lipid-mediated gene transfer to primary tumors following systemic administration, *Gene Ther.* 7 (2000) 1833–1839.
- [14] G. Zhang, X. Gao, Y.K. Song, R. Vollmer, D.B. Stolz, J.Z. Gasiorowski, D.A. Dean, D. Liu, Hydroporation as the mechanism of hydrodynamic delivery, *Gene Ther.* 11 (2004) 675–682.
- [15] Y. Negishi, Y. Endo, T. Fukuyama, R. Suzuki, T. Takizawa, D. Omata, K. Maruyama, Y. Aramaki, Delivery of siRNA into the cytoplasm by liposomal bubbles and ultrasound, *J. Control. Release* 132 (2008) 124–130.
- [16] I. Lentacker, N. Wang, R.E. Vandenbroucke, J. Demeester, S.C. De Smedt, N.N. Sanders, Ultrasound exposure of lipoplex loaded microbubbles facilitates direct cytoplasmic entry of the lipoplexes, *Mol. Pharm.* 6 (2009) 457–467.
- [17] K. Un, S. Kawakami, R. Suzuki, K. Maruyama, F. Yamashita, M. Hashida, Development of an ultrasound-responsive and mannose-modified gene carrier for DNA vaccine therapy, *Biomaterials* 31 (2010) 7813–7826.
- [18] K. Un, S. Kawakami, R. Suzuki, K. Maruyama, F. Yamashita, M. Hashida, Suppression of melanoma growth and metastasis by DNA vaccination using an ultrasound-responsive and mannose-modified gene carrier, *Mol. Pharm.* 8 (2011) 543–554.
- [19] K. Un, S. Kawakami, M. Yoshida, Y. Higuchi, R. Suzuki, K. Maruyama, F. Yamashita, M. Hashida, The elucidation of gene transferring mechanism by ultrasound-responsive unmodified and mannose-modified lipoplexes, *Biomaterials* 32 (2011) 4659–4669.
- [20] T. Pazmany, S.P. Murphy, S.O. Gollnick, S.P. Brooks, T.B. Tomasi, Activation of multiple transcription factors and fos and jun gene family expression in cells exposed to a single electric pulse, *Exp. Cell Res.* 221 (1995) 103–110.
- [21] M. Nishikawa, A. Nakayama, Y. Takahashi, Y. Fukuhara, Y. Takakura, Reactivation of silenced transgene expression in mouse liver by rapid, large-volume injection of isotonic solution, *Hum. Gene Ther.* 19 (2008) 1009–1020.
- [22] H. Mukai, S. Kawakami, H. Takahashi, K. Satake, F. Yamashita, M. Hashida, Key physiological phenomena governing transgene expression based on tissue pressure-mediated transfection in mice, *Biol. Pharm. Bull.* 33 (2010) 1627–1632.
- [23] T. Tanos, M.J. Marinissen, F.C. Leskow, D. Hochbaum, H. Martinetto, J.S. Gutkind, O.A. Coso, Phosphorylation of c-Fos by members of the p38 MAPK family. Role in the AP-1 response to UV light, *J. Biol. Chem.* 280 (2005) 18842–18852.
- [24] S. Ramanan, M. Kooshki, W. Zhao, F.C. Hsu, M.E. Robbins, PPARalpha ligands inhibit radiation-induced microglial inflammatory responses by negatively regulating NF-kappaB and AP-1 pathways, *Free Radic. Biol. Med.* 45 (2008) 1695–1704.
- [25] Y.C. Chiu, T.H. Huang, W.M. Fu, R.S. Yang, C.H. Tang, Ultrasound stimulates MMP-13 expression through p38 and JNK pathway in osteoblasts, *J. Cell. Physiol.* 215 (2008) 356–365.
- [26] S. Zhou, M.G. Bachem, T. Seufferlein, Y. Li, H.J. Gross, A. Schmelz, Low intensity pulsed ultrasound accelerates macrophage phagocytosis by a pathway that requires actin polymerization, Rho, and Src/MAPKs activity, *Cell. Signal.* 20 (2008) 695–704.
- [27] H. Ochiai, M. Fujimuro, H. Yokosawa, H. Harashima, H. Kamiya, Transient activation of transgene expression by hydrodynamics-based injection may cause rapid decrease in plasmid DNA expression, *Gene Ther.* 14 (2007) 1152–1159.
- [28] R. Eferl, E.F. Wagner, AP-1: a double-edged sword in tumorigenesis, *Nat. Rev. Cancer* 3 (2003) 859–868.
- [29] N.D. Perkins, Integrating cell-signalling pathways with NF-kappaB and IKK function, *Nat. Rev. Mol. Cell Biol.* 8 (2007) 49–62.
- [30] S.G. Pereira, F. Oakley, Nuclear factor-kappaB1: regulation and function, *Int. J. Biochem. Cell Biol.* 40 (2008) 1425–1430.
- [31] A. Cloutier, T. Ear, O. Borissevitch, P. Larivée, P.P. McDonald, Inflammatory cytokine expression is independent of the c-Jun N-terminal kinase/AP-1 signaling cascade in human neutrophils, *J. Immunol.* 171 (2003) 3751–3761.
- [32] A.M. Elsharkawy, D.A. Mann, Nuclear factor-kappaB and the hepatic inflammation-fibrosis-cancer axis, *Hepatology* 46 (2007) 590–597.
- [33] T. Takagi, M. Hashiguchi, R.I. Mahato, H. Tokuda, Y. Takakura, M. Hashida, Involvement of specific mechanism in plasmid DNA uptake by mouse peritoneal macrophages, *Biochem. Biophys. Res. Commun.* 245 (1998) 729–733.
- [34] K. Un, S. Kawakami, R. Suzuki, K. Maruyama, F. Yamashita, M. Hashida, Enhanced transfection efficiency into macrophages and dendritic cells by a combination method using mannosylated lipoplexes and bubble liposomes with ultrasound exposure, *Hum. Gene Ther.* 21 (2010) 65–74.
- [35] H. Mukai, S. Kawakami, Y. Kamiya, F. Ma, H. Takahashi, K. Satake, K. Terao, H. Kotera, F. Yamashita, M. Hashida, Pressure-mediated transfection of murine spleen and liver, *Hum. Gene Ther.* 20 (2009) 1157–1167.



Contents lists available at SciVerse ScienceDirect

International Journal of Pharmaceutics

journal homepage: www.elsevier.com/locate/ijpharm

A facile preparation method of a PFC-containing nano-sized emulsion for theranostics of solid tumors

Kouichi Shiraishi^a, Reiko Endoh^a, Hiroshi Furuhashi^a, Masamichi Nishihara^b, Ryo Suzuki^c, Kazuo Maruyama^c, Yusuke Oda^c, Jun-ichiro Jo^d, Yasuhiko Tabata^d, Jun Yamamoto^e, Masayuki Yokoyama^{a,*}

^a Medical Engineering Laboratory, Research Center for Medical Science, The Jikei University School of Medicine, 3-25-8, Nishi-shinbashi, Minato-ku, Tokyo 105-8461, Japan

^b International Institute for Carbon-Neutral Energy Research (I²CNER), Kyushu University, 744 Motoooka, Nishi-ku, Fukuoka 819-0395, Japan

^c Department of Biopharmaceutics, School of Pharmaceutical Sciences, Teikyo University, 1091-1 Suwarashi, Midori-ku, Sagami-hara, Kanagawa 252-5195, Japan

^d Department of Biomaterials, Institute for Frontier Medical Sciences, Kyoto University, 53 Kawara-cho Shogoin, Sakyo-ku, Kyoto 606-8507, Japan

^e Division of Physics and Astronomy, Graduate School of Science, Kyoto University, Kitashirakawa Oiwake-cho, Sakyo-ku, Kyoto 606-8502, Japan

ARTICLE INFO

Article history:

Received 14 June 2011

Received in revised form 27 August 2011

Accepted 2 October 2011

Available online xxx

Keywords:

Theranostics
Tumor targeting
Ultrasound
Perfluorocarbon
Emulsion

ABSTRACT

Theranostics means a therapy conducted in a diagnosis-guided manner. For theranostics of solid tumors by means of ultrasound, we designed a nano-sized emulsion containing perfluoropentane (PFC5). This emulsion can be delivered into tumor tissues through the tumor vasculatures owing to its nano-size, and the emulsion is transformed into a micron-sized bubble upon sonication through phase transition of PFC5. The micron-sized bubbles can more efficiently absorb ultrasonic energy for better diagnostic images and can exhibit more efficient ultrasound-driven therapeutic effects than nano-sized bubbles. For more efficient tumor delivery, smaller size is preferable, yet the preparation of a smaller emulsion is technically more difficult. In this paper, we used a bath-type sonicator to successfully obtain small PFC5-containing emulsions in a diameter of ca. 200 nm. Additionally, we prepared these small emulsions at 40 °C, which is above the boiling temperature of PFC5. Accordingly, we succeeded in obtaining very small nano-emulsions for theranostics through a very facile method.

© 2011 Elsevier B.V. All rights reserved.

1. Introduction

'Theranostics', 'theranosis', or 'theragnosis' is a newly created term in the fields of imaging diagnosis and drug delivery systems. As a word, 'theranostics' (Chen, 2011; Lammers et al., 2010, 2011; MacKay and Li, 2010) is a combination of therapy and diagnosis, and is defined as therapy conducted in a diagnosis-guided manner. A typical example of theranostics is found in a carrier system containing both a contrast agent for diagnosis and a drug for therapy. Theranostics has been studied with various types of drug carriers including liposomes (Kamaly and Miller, 2010), small molecules (Kalber et al., 2011), nano-particles (Jeong et al., 2011; Kim et al., 2010), emulsions (Gianella et al., 2011), synthetic polymers (Bryson et al., 2009), polymeric micelles (Blanco et al., 2009; Kaida et al., 2010; Min et al., 2010; Nakamura et al., 2006; Shiraishi et al., 2009,

2010), and other nano-sized carrier systems (Ai, 2011; Moon et al., 2011; Pan et al., 2008; Sanson et al., 2011). Ultrasound is considered to be a preferable modality for theranostics because ultrasound has been well studied and developed for image diagnoses and local therapies such as ultrasound lithotripsy and hyperthermia.

For theranostics of solid tumors, micron-sized bubbles (microbubbles) (Hernot and Klivanov, 2008; Schutt et al., 2003; Unger et al., 2004) have been actively studied because the bubbles provide strong contrasts in ultrasonic images, and because cavitation of microbubbles (Grishenkov et al., 2009) induced by ultrasound can effectively damage cells. Cells can be damaged by both jet-stream and heat that are generated in the bubbles' cavitation. In the design of microbubbles for tumor applications, the size of the microbubbles is a very important factor. Larger microbubbles can produce stronger ultrasound image contrasts. In contrast, smaller bubbles are preferred for efficient delivery into tumor tissues because the size of the trans-vascular passage from the blood-stream into the tumor interstitial space is of a diameter smaller than 1 μm. It is believed that the maximum diameter for efficient translocation into tumor tissues is 200–400 nm (Ishida et al., 1999; Litzinger et al., 1994; Nagayasu et al., 1996; Yuan et al., 1995). (In this diameter range, bubbles must be called nano-bubbles.) This is an essential dilemma concerning the size of bubbles used for

Abbreviations: PFC, perfluorocarbon; PFC5, perfluoropentane; PFC6, perfluorohexane; DBU, 1,8-diazabicyclo[5.4.0]undec-7-ene; PEG-P(Asp(C7F9)_x), poly(ethylene glycol)-*b*-poly(4,4,5,5,6,6,7,7,7-nonafluoroheptyl aspartate) block copolymer.

* Corresponding author. Tel.: +81 3 3433 1111x2336; fax: +81 3 3459 6005.

E-mail address: masajun2093ryo@jikei.ac.jp (M. Yokoyama).

0378-5173/\$ – see front matter © 2011 Elsevier B.V. All rights reserved.

doi:10.1016/j.ijpharm.2011.10.006

Please cite this article in press as: Shiraishi, K., et al., A facile preparation method of a PFC-containing nano-sized emulsion for theranostics of solid tumors. *Int J Pharmaceut* (2011), doi:10.1016/j.ijpharm.2011.10.006

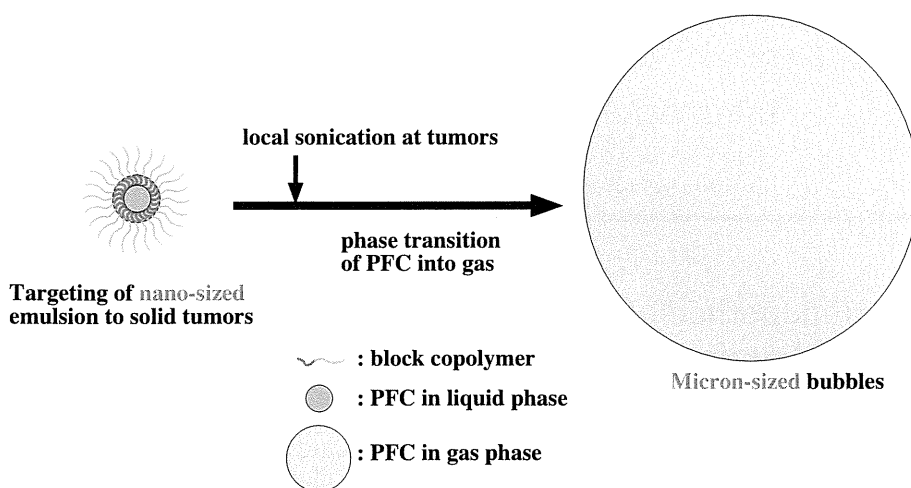


Fig. 1. Concept of phase-transition type nano-emulsion.

tumor theranostics. In order to resolve this dilemma, Kawabata et al. (Asami et al., 2009, 2010; Kawabata et al., 2005, 2010a,b) and Rapoport et al. (Mohan and Rapoport, 2010; Rapoport et al., 2007, 2009a, 2009b, 2010a,b, in press) examined nano-emulsions incorporating a specific kind of perfluorocarbon, as illustrated in Fig. 1. A boiling temperature of this perfluorocarbon (perfluoropentane, PFC5) is 29 °C, which is lower than normal human body temperature, but the integrity of these nano-emulsions is maintained owing to interfacial excessive pressure called Laplace pressure (Rapoport et al., 2009a). Upon ultrasound irradiation, the integrity of these nano-emulsions is broken, and this liquid perfluorocarbon exhibits a phase-transition into gas. Accordingly, the nano-emulsions change into microbubbles. Efficient delivery into tumor tissues is attained with the nano-emulsions, and then local sonication at the tumor tissues generates the microbubbles from the nano-emulsions, resulting in high imaging and therapeutic efficiencies. This phase-transition type nano-emulsion may be an ideal system for the theranostics of solid tumors.

Generally, preparations of smaller emulsions in a nano-meter range are more difficult because a higher power input is required in the emulsion preparations. (Tadros et al., 2004) Previously, we had prepared perfluorocarbon-containing emulsions by means of vigorous mechanical stirring with a magnetic stirrer and obtained emulsions of ca. 600 nm in diameter (Nishihara et al., 2009). In this paper, we have tried to obtain much smaller emulsions by means of ultrasound irradiation as well as high-pressure emulsification. Another important parameter for preparations of the phase-transition type nano-emulsion is temperature. A boiling temperature (29 °C) of perfluoropentane (PFC5) is close to the room temperature; therefore, preparations must be carried out at a low temperature and in a small scale for evasion of evaporation of PFC5 because heat generated in emulsification or sonication processes must be efficiently removed for the evasion. We want to find a facile preparation method that can be carried out at either room or a higher temperature, and that can be easily scaled up because the heat removal is a much less serious concern than the conventional method. Rapoport et al. (Rapoport et al., 2010b) reported preparations of nano-bubbles by means of ultrasound irradiation (with a probe type sonicator at 20 kHz) in ice-cold water. They obtained nano-emulsions of ca. 600 nm in diameter.

In this paper, we have tried to obtain very small nano-emulsions containing PFC5 by using an inexpensive bath-type sonicator (usually used as an ultrasonic cleaner) at room temperature or higher. For this emulsion preparation, we synthesized fluorinated block copolymers and optimized their compositions.

2. Materials and methods

2.1. Materials

We purchased perfluoropentane (PFC5) and perfluorohexane (PFC6) from Stream Chemicals (Newburyport, MA, USA) and Alfa Aesar (Ward Hill, MA, USA), respectively, and used them as received. We purchased 4,4,5,5,6,6,7,7,7-nonafluoroheptyl iodide from Sigma–Aldrich (Tokyo branch, Japan) and used it as received. We purchased reagent-grade solvents, dehydrated *N,N*-dimethylformamide (DMF), dimethyl sulfoxide (DMSO), and diethyl ether from Wako Chemicals (Tokyo, Japan), and used them as received. Poly(*L*-lactic acid)-grafted gelatin was prepared through a coupling reaction between a primary amine group of gelatin and a terminal hydroxyl group of the poly(*L*-lactic acid) by the use of disuccinimidyl carbonate according to a published synthetic procedure. (Tanigo et al., 2010) Poly(ethylene glycol)-block-poly(*L*-lactic acid) block copolymer (PEG-*b*-PLA) was purchased from Sigma–Aldrich (Tokyo branch, Japan). The average molecular weights of the PEG block and the PLA block were 750 and 1,000, respectively.

2.2. Block copolymer synthesis

Poly(ethylene glycol)-*b*-poly(4,4,5,5,6,6,7,7,7-nonafluoroheptyl aspartate) block copolymers (PEG-P(Asp(C7F9)*x*)) were prepared by means of esterification of the aspartic units of poly(ethylene glycol)-*b*-poly(aspartic acid) block copolymer (PEG-P(Asp)) by the use of an iodinated compound, as shown in Fig. 2. PEG-P(Asp) was synthesized according to our previous paper (Yamamoto et al., 2007). A value *x* in the PEG-P(Asp(C7F9)*x*) formula denotes mol.% of the esterified units. This esterification reaction was carried out with a corresponding iodinated compound in the presence of a super base according to a previously reported procedure (Opanasopit et al., 2004; Yokoyama et al., 2004; Yamamoto et al., 2007) with a slight modification.

The starting material was poly(ethylene glycol)-*b*-poly(aspartic acid) block copolymer (PEG-P(Asp)). The average molecular weight of PEG was 5200 (*n*=119 in Fig. 2), and the average number of Asp units per one chain was 26.0. The aspartate amide bond can be either α or β , and our group previously had reported that a ratio of α : β was 1:3 (=a:b in Fig. 2) (Yokoyama et al., 2004). PEG-P(Asp) (2.001 g, containing 6.33×10^{-3} mol Asp residue) was dissolved in 20 mL of DMF. To this mixture, was added both 4.904 g of 4,4,5,5,6,6,7,7,7-nonafluoroheptyl iodide (which is

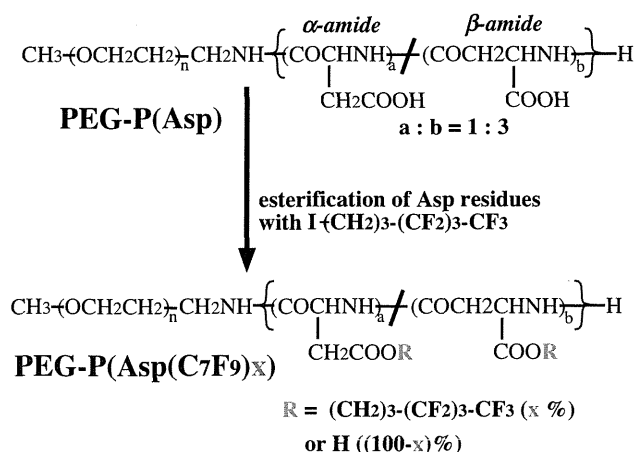


Fig. 2. Synthesis of the fluorocarbon-containing block copolymer PEG-P(Asp(C7F9))_x.

2.00 mol. equivalents to the Asp residue, I-(CH₂)₃-(CF₂)₃-CF₃ in Fig. 2) and 0.972 g of 1,8-diazabicyclo[5.4.0]undec-7-ene (DBU, which is 1.01 mol. equivalents to the Asp residue). DBU is a very strong base, and can induce ionization in a carboxyl group of the aspartic acid residue in an organic solvent, DMF. The reaction mixture was heated at 50 °C for 16 h. An ester formed at the Asp residue through a nucleophilic substitution reaction of the ionized carboxyl group with I-(CH₂)₃-(CF₂)₃-CF₃. After this 16-h reaction, the reaction mixture was poured into 200 mL of ice-cold diethyl ether for precipitation of the polymer. The precipitated polymer was filtered and washed with diethyl ether. The obtained polymer was dissolved in 20 mL of DMSO, to which was added 2.11 mL of 6N hydrochloric acid. This acid works for removal of DBU from polymers. This polymer solution was dialyzed with a Spectra/Por 6 dialysis membrane (molecular weight cut-off is 1000) against DMSO for 2 days and against milliQ water for an additional 2 days, followed by freeze-drying. Yield was 2.436 g. To determine the contents of the fluorinated ester group of the polymer, we used ¹H NMR spectroscopy in DMSO-d₆ containing 3 v/v% trifluoroacetic acid. For this determination, we identified a peak area ratio between the methylene protons (-COOCH₂CH₂CH₂CF₂CF₂CF₂CF₃) at 1.8 ppm of the ester group and the methylene protons (-OCH₂CH₂-) at 3.6 ppm of the PEG block. The esterification percentage (x in Fig. 2) was revealed to be 59%. The other compositions of block copolymers were synthesized according to the same method with various molar ratios of I-(CH₂)₃-(CF₂)₃-CF₃ and DBU with respect to the aspartic acid residue. Table 1 lists all the compositions of the synthesized block copolymers.

Table 2

Effects of polymer composition and sample volume on PFC5 incorporation behaviors.

Run	Polymer	Sample volume (μL)	PFC5 concentration (vol.%) ^a	Cumulant average diameter (nm) ^a
1	F-6%	300	0.840 ± 0.097	261.2 ± 3.4
2	F-15%	300	0.948 ± 0.131	232.4 ± 14.5
3	F-39%	300	0.625 ± 0.074	198.4 ± 33.3
4	F-59%	300	0.669 ^b	133.9 ^b
5	F-67%	300	0.682 ± 0.060	222.8 ± 37.9
6	F-59%	300	0.682 ± 0.074	205.5 ± 15.8
7	F-59%	300	0.634 ± 0.361	173.5 ± 24.5
8	F-59%	700	1.110 ^b	231.8 ^b
9	F-59%	1200	1.792 ^b	280.6 ^b

^a Average ± standard deviation (n = 3) except runs 4, 8, and 9.

^b Average of two preparations.

Table 1

Compositions of PEG-P(Asp(C7F9))_x.

Code	M.W. of PEG	Asp unit number (n)	Esterification degree (x%)
F-6%	5200	22.1	5.9
F-15%	5200	23.3	14.6
F-39%	5200	22.1	38.5
F-59%	5200	26.0	58.5
F-67%	5200	22.1	67.0

2.3. Preparation of PFC-containing nano-emulsions

We examined preparations of PFC5-containing nano-emulsions according to two methods using a high-pressure emulsifier and a bath-type sonicator.

2.3.1. Preparation with a high-pressure emulsifier

We dissolved PEG-P(Asp(C7F9))₁₅ block copolymer by stirring it in distilled water at a concentration of 4.0 wt. % of the solution, and added perfluoropentane (PFC5) and perfluorohexane (PFC6) at each 1.25 vol.% of the solution. We vigorously stirred the solution with a homogenizer Polytron (Kinematica AG, Tokyo, Japan) at 25,000 rpm for 10 s. Then, we conducted emulsification using a high-pressure emulsifier EmulsiFlex-C5 CSC (AVESTIN, Inc., Ottawa, Ontario, Canada) at 4 °C for 6 min at ca. 50 MPa. We collected a white emulsion, and filtered it with a Sartorius Minisart (R) filter (1.2 μm pore, Sartorius AG, Göttingen, Germany).

2.3.2. Preparation with a bath-type sonicator

We dissolved PEG-P(Asp(C7F9))_x block copolymers in MilliQ water at a concentration of 1.0 to 4.0 wt.% of water. In case of a high ester content such as x = 59, we heated (up to ca. 40 °C) and sonicated the solutions until we obtained a transparent polymer solution. The polymer solution was transferred to a 1.5-mL glass vial that was sealed with a Teflon-silicon rubber cap (Chromacol auto-sampler vial 2-SV for HPLC; GL Science, Inc., Tokyo, Japan), and was cooled on ice. Then, we added perfluoropentane (PFC5) and perfluorohexane (PFC6) at 0.5–4.0 vol.% of water. We confirmed PFCs' position at the bottom of the solution. (Sometimes PFCs, whose densities are much greater than water's, did not go into the aqueous solution. Therefore, we shook the vial vigorously to allow PFC droplets to sink to the bottom by force of gravity.) Then, we sealed the vial with a cap, and applied sonication for 3 min with a bath-type sonicator Branson model 1510 (oscillating frequency at 42 kHz, max. power intensity: 90 W, Danbury, CT, USA). The temperature of the bath was kept constant with degassed cold and hot water. In all the sonication procedures, we had a constant water level in a sonicator bath and a fixed position of the vial in order to obtain sonication conditions that were as identical to one another as possible. Finally, we collected a supernatant by leaving unincorporated PFC droplets at the bottom.

In order to measure amounts of the polymer chains that were not included in the PFC-emulsions, we carried out the following experiment. PFC-emulsion was prepared in the conditions of Run 4 of Table 2; polymer: F-59%, sample volume: 300 μ L, polymer concentration: 4 wt.%, PFC5: 2 vol.%, PFC6: 2 vol.%, sonication at 40 °C for 3 min. The obtained emulsion was transferred into a 1.5 mL Eppendorf-type poly(propylene) tube and centrifuged at 13,200 rpm for 5 min with an Eppendorf centrifuge model 5415D (Eppendorf Co., Ltd. Japan, Tokyo, Japan). The emulsion was found to precipitate at the bottom. 200 μ L of the supernatant was collected and freeze-dried. We calculated the polymer amounts that were not included in the PFC-emulsions by multiplying 1.5 (=300 μ L/200 μ L) to the freeze-dried polymer weight. As a control, we carried out the same experiment just only for the polymer (without addition of TFC5 nor TFC6).

2.4. Measurements

2.4.1. Dynamic light scattering (DLS)

The size of emulsions was measured with a dynamic light scattering (DLS) instrument, the DLS-7000 (Otsuka Electronics, Tokyo, Japan). DLS samples were prepared through appropriate dilution of the emulsions with commercial distilled water for internal injection (Otsuka Pharmaceutical Co. Ltd., Tokyo, Japan). The measurements were made at 25 °C, and scattering was observed at a 90° angle with respect to the incident beam. The cumulant average particle size and the particle size distribution from a non-negative least square method were determined by the use of software provided with the instrument.

2.4.2. Gas chromatography

We measured concentrations of PFC5 using two gas chromatograph systems as described below. In both cases, we successfully obtained clear separation of PFC5's peak from PFC6's peak, and carried out quantitative analyses using a standard sample of PFC5. Therefore, the two gas chromatograph systems gave us identical results. However, we only used the (2) system described below for blood samples because its pre-heating function was essential for measurements of blood samples.

2.4.2.1. Gas chromatograph system. We measured PFC5 using a gas chromatograph model G-6000 (Hitachi High-Technologies Corporation, Tokyo, Japan) equipped with a Gaskuropack 54 80/100 packed column (GL Sciences, Inc., Tokyo, Japan) and an FID detector at 200 °C. Carrier gas was nitrogen at a flow rate of 300 mL/min. 5 μ L of a sample solution were injected into the gas chromatograph system with a micro syringe at 0 min. Column temperature was controlled in the following manner; 100 °C (0 min), raised at a rate of 5 °C/min until 130 °C (6 min), and then raised at a rate of 60 °C/min until 190 °C (7 min), followed by maintenance of 190 °C for 2 min. PFC5 and PFC6 were found to elute at 3.8 min and 6.4 min, respectively.

2.4.2.2. Gas chromatograph system. We measured PFC5 using a gas chromatograph system GC-2014 (Shimadzu Corp., Kyoto, Japan) equipped with an FID detector at 250 °C. We used two tandem-connected two columns: DB-WAX 127-7012 (Agilent Technologies Japan, Ltd., Tokyo, Japan) and RESTEK Rt-QBond 19741 (Shimadzu GLC Ltd., Tokyo, Japan). Carrier gas was helium at a flow rate of 20 mL/min. Either 100 or 544 μ L of a sample solution were heated at 200 °C and injected with a headspace autosampler TurboMatrix Trap 40 (PerkinElmer Japan Co., Ltd., Yokohama, Japan). Column temperature was constant at 150 °C. PFC5 and PFC6 were found to elute at 3.6 min and 4.4 min, respectively.

2.5. Measurements of PFC5 concentration in blood

In vivo PFC5 concentration profiles in blood were evaluated in Balb/c female mice (6 weeks old). 100 μ L of PFC-emulsion was intravenously administered via lateral tail veins. The emulsions' PFC5 concentrations ranged from 0.429 to 0.670 vol.%. Blood (44 μ L) was collected with a heparinized blood-collecting glass tube, and mixed with 500 μ L of heparin solution in a capped sample tube of the (2) gas chromatograph system.

3. Results

3.1. General characteristics of the emulsion-preparation method with a bath-type sonicator

In representative conditions, we successfully obtained PFC5-containing nano-sized emulsions having diameters of ca. 200 nm in considerably high PFC5 yields. Fig. 3(a) and (b) shows diameter distributions measured by means of dynamic light scattering (DLS) for PEG-P(Asp(C7F9)59) (F-59% in Table 1). In these conditions, we dissolved 12.0 mg of polymer in 300 μ L water (4.0 wt.% solution), and put this polymer solution in a 1.5 mL glass vial, followed by additions of 6 μ L (corresponding to 2.0 vol.% of water) of PFC5 and 6 μ L of PFC6. Sonication was performed for 3 min in a bath-type sonicator at 40 °C. In the first three preparations (run 6 in Table 2), the cumulant diameter obtained was 205.5 \pm 15.8 nm (the average \pm standard deviation; $n=3$), and Fig. 3(a) shows the weight-weighted diameter distribution of one preparation. Almost uniformly distributed emulsions were obtained, and the diameter of the emulsion droplets had a very small size about 200 nm. In this run 6, PFC5 concentrations were 0.682 \pm 0.074 vol.%. These values are considered large enough for ultrasound images (Kawabata et al., 2005, 2010a,b). In another set of three preparations (on another day, run 7 in Table 2), we obtained a very similar average diameter, 173.5 \pm 24.5 nm (the average \pm standard deviation; $n=3$) and PFC5 concentrations. The diameter distribution of one preparation of run 7 is shown in Fig. 3(b). These two figures exhibited a major peak at about 200 nm, while a minor peak was seen in a larger diameter side and a smaller diameter side, as shown in Fig. 3(a) and (b), respectively. This difference may result from a slight variation in sonication conditions such as the position of samples and the water level of the sonicator. These emulsions were obtained and measured without any purification process after the sonication, and a large majority of the emulsions in weight were found to have a diameter of about 200 nm. All these results clearly indicate that this sonication method brought about very small nanometer-sized PFC5-containing emulsions with considerably high PFC5 concentrations.

We measured a proportion of polymer incorporated in the PFC-emulsion out of the feed polymer amount. In these preparation conditions (run 7 in Table 2), 75.4 \pm 2.6% ($n=3$) of the feed polymer was found in a supernatant obtained after centrifugation. (All the PFC-emulsions were observed to precipitate in this centrifugation.) When this measurement was carried out for the polymer alone, 93.8 \pm 2.0% ($n=3$) of the feed polymer was found in a supernatant obtained after centrifugation. Therefore, 18.4% (=93.8%–75.4%) of the feed polymer was considered to be incorporated into the PFC-emulsions. Removal of the free polymer chain, that was not incorporated into the PFC-emulsion, was not examined in this study. The removal is difficult because the free polymer existed as a polymeric micelle was close to the PFC-emulsion in size. (If the free polymer existed as a single polymer chain, a difference in size between the free polymer and the PFC-emulsion would be so large to allow separation such as ultrafiltration.)

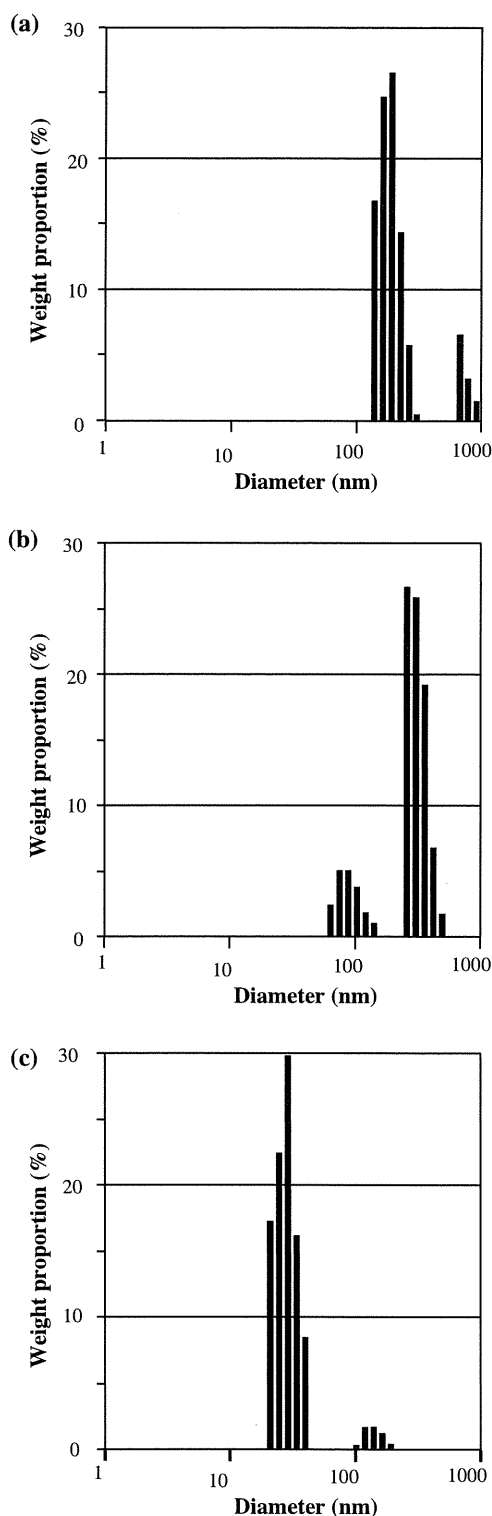


Fig. 3. Diameter distribution of PFC5-containing nano-emulsions (a and b) forming from PEG-P(Asp(C7F9)59) and empty polymeric micelle (c) measured by means of DLS. (a and b) are of different batches but prepared in the same conditions.

Using this polymer amount incorporated into the PFC-emulsions, we calculated the thickness of the polymer shell. We carried out the calculation with the following assumptions.

- (1) The PFC-emulsions are made of the two phases; the inner PFC droplet phase and the outer polymer shell phase.
- (2) We obtained PFC6 amounts in the emulsions assuming that sensitivity of PFC6 in gas chromatography is the same as that of PFC5. (The same peak area per PFC volume.)
- (3) PFC6 and PFC5 are mixed freely without any gain or loss of droplet volume.
- (4) Density of polymer is 1.03. (This is a common value of protein, and most synthetic polymers show similar values.)

The obtained value of the polymer shell's thickness was 22 nm, while the radius of the PFC droplet was 65 nm. In the future study, we like to analyse relationships between the shell thickness and physical stability of the emulsions.

3.2. Comparison with other emulsion-preparation methods

We compared the PFC5's concentrations of the PFC5-containing emulsions prepared in the sonication method with the PFC5's concentrations of the emulsions prepared in two common methods; mechanical stirring and high-pressure emulsification (Solans et al., 2005). We also compared the diameters of the emulsions prepared in the sonication method with those prepared in the two common methods. Previously, we reported PFC5-containing emulsions prepared by means of mechanical stirring that featured a magnetic stirrer (Nishihara et al., 2009). In this method, only the F-14% polymer provided a high PFC5 concentration (0.65 vol.%). The other polymers provided low or very low PFC5 concentrations: F-6% had 0.28 vol.%, F-22% had 0.19 vol.%, F-39% had 0.02 vol.%, and F-67% had 0.01 vol.%. In the F-14% case, the cumulant diameter was 694 nm, which was much larger than those obtained in the sonication method as described in the previous section (Section 3.1). Another distinct difference was found in a wide range of polymer compositions for high PFC5 concentrations in the sonication method. As summarized in runs 1–5 of Table 2, we compared the PFC5 concentrations (vol.%) and average diameters of the PFC5-containing emulsions for five polymer compositions. All these five compositions of polymers provided high PFC5 concentrations larger than 0.6 vol.%. Furthermore, all emulsion sizes of these runs (runs 2–5) were revealed to be small, at about 200 nm.

In the next step, we compared the sonication method with the most common method for emulsion preparation: high-pressure emulsification. For this comparison, we used F-15% polymer. We compared PFC5 concentrations and the cumulant average diameters of the emulsions prepared in the sonication method with PFC5 concentrations and the cumulant average diameters of the "high-pressure method" emulsions. We acquired a considerably high PFC5 concentration, 0.58 vol.%, by using a high-pressure emulsifier for the high-pressure emulsification method (its procedure is described in Section 2.3.1). However, the cumulant average diameter of the obtained emulsion was 477 nm. This value was much larger than the sonication-method value (232.4 nm, run 2 of Table 2). Additionally, maintenance of a low temperature at 4 °C for the whole instrument was essential in the high-pressure emulsification method, since possible heat generation due to the high-pressure process may considerably boost evaporation of PFC5 (the boiling temperature of PFC5 is 29 °C). In contrast, in the sonication method, a high PFC5 concentration was obtained at 40 °C, which is above PFC5's boiling temperature. (The temperature issue of the emulsion-preparation process will be more closely examined in the following section (Section 3.4).)

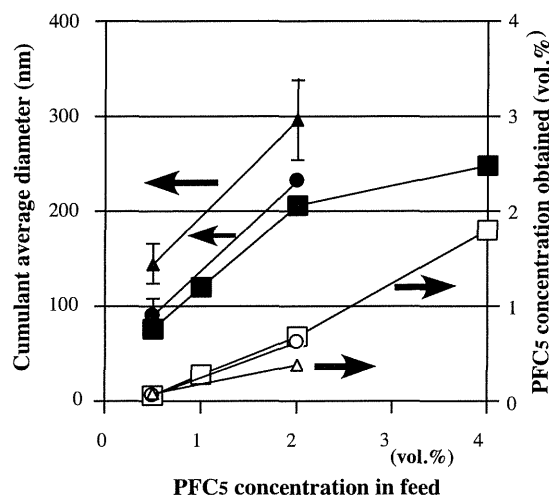


Fig. 4. Effects of polymer and PFC5 concentrations on physical properties of emulsions. PEG-P(Asp(C7F9)59) was used for emulsion preparations. Sample volume was 300 μL in 1.5-mL sample vials. Sonication was performed for 3 min at 40 $^{\circ}\text{C}$. Filled plots represent cumulant average diameters, and vacant plots represent PFC5 concentrations of emulsions. Polymer concentration: Δ , \blacktriangle : 1.0 vol.%; \circ , \bullet : 2.0 vol.%; \square , \blacksquare : 4.0 vol.%.

All these results indicate that the sonication method is a facile method for preparations of PFC5-containing emulsions with very small nano-sizes and high PFC5 concentrations.

3.3. Effects of sample volume, polymer concentration, and PFC5 concentration on incorporation behaviors

In the standard conditions, we put 300 μL water in a 1.5-mL of sealed glass tube and added polymer, PFC5, and PFC6. This configuration meant that a considerable amount of PFC5 perhaps would move from the solution into the glass tube's vacant atmospheric space (ca. 1.2 mL). We changed the volume of water while keeping constant the concentrations of polymer, PFC5, and PFC6 in the tube. Table 2 summarizes the results of runs 6–9 of Table 2. A higher PFC5 concentration was obtained in a case involving a larger water volume. (This means that there was a smaller vacant space in a sealed tube.) In accordance with the higher concentration of PFC5, the average diameter of the emulsion was observed to be larger. In run 9, PFC5's yield reached a very high value, approximately 90%. On the other hand, the PFC5's yield decreased to 32–33% when a small sample volume (300 μL) was adopted. These values indicate that the emulsification process can be well controlled through adjustment of sample volume.

Then, we examined effects that both polymer concentrations and PFC5 concentrations in feed had on the two physical values: diameter and PFC5 concentrations of the emulsion. Fig. 4 shows results of these two physical values for F-59% polymer cases. We changed the polymer concentration and the PFC5 concentration in feed in a range of 1.0–4.0 wt.% and of 0.5–4.0 vol.%, respectively. Each empty plot indicates PFC5 concentrations obtained for each polymer concentration, while each filled plot indicates cumulant average diameters for each polymer concentration. The polymer concentration was not found to significantly affect these two physical values. The polymer concentration affected very slightly the PFC5 content because three plot lines almost overlapped. When the polymer concentration was raised, only a small drop in the cumulant average diameter was observed. In contrast, the PFC5 concentration in feed was revealed to greatly affect the two physical values; larger values of PFC5 concentrations and cumulant average diameters were obtained with larger PFC5 concentrations in

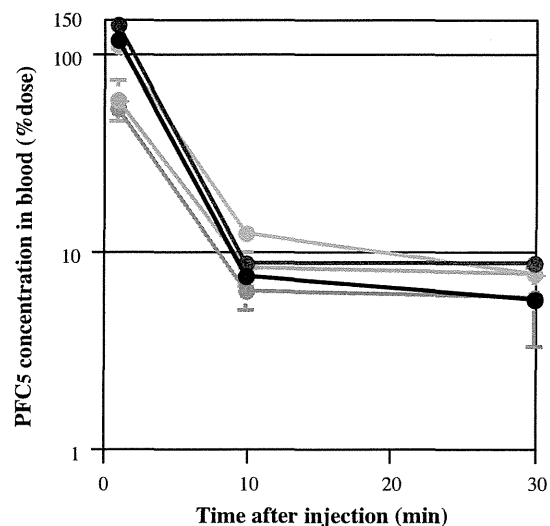


Fig. 5. Profiles of PFC5 concentration in blood. Black plot: run 1; blue plot: run 2; green plot: run 3; yellow plot: run 4; and red plot: run 5 (Table 5).

feed. Diameters of multi-modal distributions like Fig. 3(a) and (b) cannot be evaluated with the cumulant average diameters because the cumulant average diameters suppose the uni-modal diameter distribution. Therefore, we evaluated weight-weighted diameter distributions. Supplementary data, Table A summarizes and compares weight-weighted diameters with the cumulant average diameters. In most emulsion preparations, diameter distributions were found to be bi- or tri-modal, and therefore, exactly quantitative measurements of weight-weighted diameters are difficult in the homodyne analysis of dynamic light scattering done in this study. In fact, considerable differences are observed between the weight-weighted diameters and the cumulant average diameters for emulsions prepared in low PFC5 feed concentrations such as 1%, possibly due to the presence of empty polymeric micelles. (A DLS result of the empty micelle is shown in Fig. 3(c).) Even in this technical difficulty, the correlations obtained in Fig. 4a are not changed when multi-modal distributions are compared in the Supplementary data, Table A.

From the results obtained in this section, it was revealed that the sample volume and the PFC5 concentration in feed were appropriate factors for the facile control of size and the PFC5 content of the nano-sized emulsion.

3.4. Function of PFC6 in an emulsion preparation

In the above-described procedures for the emulsion preparation, we always used a 1:1 (vol./vol.) mixture of PFC5 and PFC6 in order to obtain a high PFC5 yield at a temperature higher than the boiling temperature of PFC5. We chose this 1:1 ratio because Kawabata et al. reported that ultrasound intensity required for the phase-transition (vaporization) induction at the 1:1 ratio was similar to that of a PFC5 alone case, and that this intensity was almost constant between ratios of 15:85, 50:50 (=1:1), and 85:15 (Asami et al., 2009). We varied temperatures (15, 25, 40, and 65 $^{\circ}\text{C}$) of a sonicator's water bath, and performed the emulsion preparation both in the presence and the absence of PFC6 at each temperature. Table 3 summarizes results. In the absence of PFC6, PFC5 concentration was smaller than that of the corresponding PFC6-present case at every temperature. In runs 2 and 4, the obtained emulsions contained a considerable quantity of PFC5 over 0.2 vol.%. These two runs were prepared at lower temperatures than a boiling temperature of PFC5 (29 $^{\circ}\text{C}$). Only a very small amount of PFC5

Table 3

Effects of temperature and PFC6 addition on PFC5 incorporation behaviors.

Run	Temperature (°C)	PFC6 addition	PFC5 concentration (vol.%) ^a	Cumulant average diameter (nm) ^a
1	15	Yes	0.727 ± 0.191	210.8 ± 17.8
2	15	No	0.419 ± 0.124	82.7 ± 2.6
3	25	Yes	0.566 ± 0.367	177.1 ± 8.9
4	25	No	0.205 ± 0.086	95.7 ± 8.9
5 ^b	40	Yes	0.634 ± 0.361	173.5 ± 24.5
6	40	No	0.049 ± 0.059	98.5 ± 5.1
7	65	Yes	0.154 ± 0.051	136.2 ± 16.0
8	65	No	0.096 ^c	303.7 ^c

^a Average ± standard deviation (n = 3) except run 8.^b This run is identical to run 6 of Table 2.^c Average of two preparations.

was incorporated in run 6, which was performed at 40 °C, which is above PFC5's boiling temperature. This indicates that most PFC5 evaporated at 40 °C, and that interfacial Laplace pressure did not suppress PFC5's evaporation in the sonication procedure possibly because PFC5 evaporated from macroscopic PFC's droplets (in mm scale) before its incorporation into nano-emulsions where Laplace pressure's effect is great. In contrast, the PFC6-present cases presented similar amounts of PFC5 incorporated at 15, 25, and 40 °C. This means that PFC5's evaporation at 40 °C was efficiently suppressed through the mixing with PFC6. PFC5 and PFC6 not only are miscible but also these two compounds are expected to strongly interact with each other because these are both perfluorocarbons. It is considered that PFC5 evades evaporation through the strong interaction with PFC6 that has a higher boiling temperature than 40 °C. In run 7, performed at 65 °C, a considerable drop in the incorporated PFC5 amount was seen. This sonication temperature (65 °C) is higher than PFC6's boiling temperature (60 °C), and therefore, both PFC5 and PFC6 were evaporated at 65 °C. From these results, we have confirmed the function of the added PFC6 for high PFC5-incorporation amounts at a temperature higher than PFC5's boiling temperature.

3.5. PFC5 concentration profile in blood

We measured PFC concentrations in blood using several PFC5-containing emulsions in order to control their pharmacokinetic behaviors. For a larger amount of emulsion accumulation at tumor tissues, a longer half-life is preferable for a contrast agent. In contrast, a shorter half-life is advantageous for a diagnosis in a short period after injection of a contrast injection, since a low concentration of the contrast agent in blood is a pre-requisite for a high contrast image of the contrast agent's accumulated region. Under this contradictory situation for the optimum half-life, it is very important to obtain technologies to control (prolong and shorten) a half-life of the contrast agent.

We used three different types of polymers including PEG-P(Asp(C7F9)x) block copolymers in order to control half-lives in blood. In Table 4, we describe the compositions of the two

Table 4

Compositions of two poly(L-lactic acid)(PLA)-containing polymers.

Code	Structure	Compositions
Gelatin derivative	Poly(L-lactic acid)-grafted gelatin	M.W. of PLA: 1000 ratio PLA/gelatin = 0.17
PEG-PLA	Poly(ethylene glycol)-b-Poly(L-lactic acid) Block copolymer	M.W. of PEG: 2000 M.W. of PLA: 1000

copolymers other than PEG-P(Asp(C7F9)x). These two copolymers contain hydrophobic poly(L-lactic acid) chains that are expected to work for incorporation of hydrophobic PFC5 into emulsions. Table 5 summarizes five samples prepared from four polymers. By adjusting the vacant volume of a 1.5-mL glass vial to a small value (ca., 300 μL, meaning 1.2 mL of the sample volume.), we successfully obtained emulsions with higher PFC5 contents than 0.4 vol.% in runs 1–3. In these cases, the sonication was carried out at 15 °C. When emulsions were prepared in the same conditions of run 1 except for a different temperature (at 40 °C) and a different vacant volume (ca. 0 μL), the PFC5 content was considerably lower (0.408 vol.%) than in run 1.

We injected these five samples in a mouse tail vein. As shown in Fig. 5, we observed a distinct difference in PFC5 concentrations at 1 min after the injection between three runs containing PLA (runs 1–3) and the other two runs for PEG-P(Asp(C7F9)x). The former three runs showed almost a 100% dose at 1 min with an assumption that blood volume was 7 vol./wt.% of body weight, while the latter two runs provided considerably smaller values than the 100% dose. In all runs, however, PFC5 concentrations were rapidly lowered at 10 and 30 min after the injection, and no clear difference was observed at these time points among all the runs. Therefore, control of pharmacokinetic behaviors, in particular prolongation of blood half-life from a few minutes, was not successfully achieved in this examination by the use of different polymer structures. For the pharmacokinetic control of the emulsions, an additional functional component may be required. Rapoport et al. (Rapoport et al., 2011) reported a very stable circulation (half-life = 2–4 h) in blood for perfluoro-crown-ether compound containing nano-emulsions.

Table 5

Compositions of PFC-emulsions for in vivo experiments.

Run	Polymer	Polymer concentration in feed (%) ^a	PFC5 concentration in feed (vol.%)	PFC5 concentration obtained in emulsion (vol.%)	Cumulant average diameter (nm)
1	Gelatin derivative ^b	1.0	1.25 ^d	0.613	345.9
2	Gelatin derivative ^b	4.0	1.25 ^d	0.429	542.6
3	PEG-b-PLA ^a	4.0	1.0 ^d	0.491	222.6
4	F-15% ^c	4.0	2.0	0.465	256.3
5	F-59% ^c	4.0	1.0	0.670	225.1

^a Weight (g)/water volume (mL).^b Listed in Table 4.^c Listed in Table 1.^d Sonication at 15 °C.

According to this report, a perfluoro compound showing stable emulsion formation may be utilized for stable incorporation of another PFC.

4. Discussion

In the examinations of this study, we successfully obtained very small (ca. 200 nm in diameter) PFC5-containing emulsions with high PFC5 contents in a very facile method using a common bath-type sonicator. Actually, the used sonicator was the smallest model with the lowest sonication power (max. Input power: 90 W) in its product line. The other facile aspect of this preparation method is the working temperature. By mixing PFC6 we performed the emulsion preparation at 40 °C, which is above the boiling temperature of PFC5. In a conventional method's use of a high-pressure emulsifier, cooling of the whole system is required for evading a large amount evaporation of PFC5 due to heat generated within a high-pressure emulsifier. In contrast, we did not need cooling samples during the preparation. This facileness is substantially important when we consider a scale-up of the emulsion preparations. In a large-scale production of these emulsions, the heat generated in preparation processes (both in emulsification and sonication) may become large enough to raise a temperature of the solution above the boiling temperature. Therefore, successful preparations at a high temperature means that there is a large margin for large-scale preparation with high PFC5 content as well as easy handling of samples at room temperature throughout the sonication procedure.

We could not substantially change pharmacokinetic behaviors of the PFC5-containing emulsion, even when using different polymers. This is a very different situation from polymeric micelle drug carrier cases where block polymer structure was revealed to be a very influential factor on pharmacokinetic behaviors of the incorporated drug into the polymeric micelles (Yokoyama, 2005, 2007; Watanabe et al., 2006). This difference may result from the liquid state of the emulsion's core, while the solid core is essential for stable drug incorporation in the polymeric micelle systems. An alternative and novel method may be required to obtain stable incorporation of liquid PFC for dramatically changed pharmacokinetics.

5. Conclusion

By using a bath-type sonicator, we successfully obtained PFC5-containing emulsions in a diameter range of 200 nm. These emulsions are very potent for theranostics of solid tumors through ultrasound irradiation. Furthermore, these emulsions were prepared in high PFC5 yields at 40 °C, which is higher than the boiling temperature of PFC5. This very facile preparation method is an important technological key for large-scale production of these medically valuable emulsions.

Acknowledgements

This work was supported by the New Energy and Industrial Technology Development Organization, Japan. M. Yokoyama, K. Shiraishi, and M. Nishihara acknowledge support from the JST CREST program, Grant-in-Aid of the Ministry of Education, Culture, Sports, Science and Technology, Japan, and Kanagawa Academy of Science and Technology. The authors acknowledge Dr. Ken-ichi Kawabata and Dr. Rei Asami of Central Research Laboratory, Hitachi, Ltd., for their valuable discussion on PFC-containing nano-emulsions.

Appendix A. Supplementary data

Supplementary data associated with this article can be found, in the online version, at doi:10.1016/j.ijpharm.2011.10.006.

References

- Ai, H., 2011. Layer-by-layer capsules for magnetic resonance imaging and drug delivery. *Adv. Drug Deliv. Rev.* 63, 772–788.
- Asami, R., Azuma, T., Kawabata, K., 2009. Fluorocarbon droplets as next generation contrast agents—their behavior under 1–3 mhz ultrasound. *IEEE Proc. Int. Ultrasonics Symp.*, 1294–1297.
- Asami, R., Ikeda, T., Azuma, T., Kawabata, K., Umemura, S., 2010. Acoustic signal characterization of phase change nanodroplets in tissue-mimicking phantom gels. *Jpn. J. Appl. Phys.* 49, 07HF16.
- Blanco, E., Kessinger, C.W., Sumer, B.D., Gao, J., 2009. Multifunctional micellar nanomedicine for cancer therapy. *Exp. Biol. Med.* 234, 123–131.
- Bryson, J.M., Fichter, K.M., Chu, W.J., Lee, J.H., Li, J., Madsen, L.A., McLendon, P.M., Reineke, T.M., 2009. Polymer beacons for luminescence and magnetic resonance imaging of DNA delivery. *Proc. Natl. Acad. Sci. U.S.A.* 106, 16913–16918.
- Chen, X.S., 2011. Introducing theranostics journal—from the editor-in-chief. *Theranostics* 1, 1–2.
- Gianella, A., Jarzyna, P.A., Mani, V., Ramachandran, S., Calcagno, C., Tang, J., Kann, B., Dijk, W.J., Thijssen, V.L., Griffioen, A.W., Storm, G., Fayad, Z.A., Mulder, W.J., 2011. A multifunctional nanoemulsion platform for imaging guided therapy evaluated in experimental cancer. *ACS Nano* 5, 4422–4433.
- Grishenkov, D., Pecorari, C., Brismar, T.B., Paradossi, G., 2009. Characterization of acoustic properties of PVA-shelled ultrasound contrast agents: ultrasound-induced fracture (part II). *Ultrasound Med. Biol.* 35, 1139–1147.
- Hernot, S., Klibanov, A.L., 2008. Microbubbles in ultrasound-triggered drug and gene delivery. *Adv. Drug Deliv. Rev.* 60, 1153–1166.
- Ishida, O., Maruyama, K., Sasaki, K., Iwatsuru, M., 1999. Size-dependent extravasation and interstitial localization of polyethyleneglycol liposomes in solid tumor-bearing mice. *Int. J. Pharm.* 190, 49–56.
- Jeong, H., Huh, M., Lee, S.J., Koo, H., Kwon, I.C., Jeong, S.Y., Kim, K., 2011. Photosensitizer-conjugated human serum albumin nanoparticles for effective photodynamic therapy. *Theranostics* 1, 230–239.
- Kaida, S., Cabral, H., Kumagai, M., Kishimura, A., Terada, Y., Sekino, M., Aoki, I., Nishiyama, N., Tani, T., Kataoka, K., 2010. Visible drug delivery by supramolecular nanocarriers directing to single-platformed diagnosis and therapy of pancreatic tumor model. *Cancer Res.* 70, 7031–7041.
- Kalber, T.L., Kamaly, N., Higham, S.A., Pugh, J.A., Bunch, J., McLeod, C.W., Miller, A.D., Bell, J.D., 2011. Synthesis and characterization of a theranostic vascular disrupting agent for in vivo MR imaging. *Bioconjug. Chem.* 22, 879–886.
- Kamaly, N., Miller, A.D., 2010. Paramagnetic liposome nanoparticles for cellular and tumour imaging. *Int. J. Mol. Sci.* 11, 1759–1776.
- Kawabata, K., Sugita, N., Yoshikawa, H., Azuma, T., Umemura, S., 2005. Nanoparticles with multiple perfluorocarbons for controllable ultrasonically induced phase shifting. *Jpn. J. Appl. Phys.* 44, 4548–4552.
- Kawabata, K., Asami, R., Yoshikawa, H., Azuma, T., Umemura, S., 2010a. Acoustic response of microbubbles derived from phase-change nanodroplet. *Jpn. J. Appl. Phys.* 49, 07HF18.
- Kawabata, K., Asami, R., Yoshikawa, H., Azuma, T., Umemura, S., 2010b. Sustaining microbubbles derived from phase change nanodroplet by low-amplitude ultrasound exposure. *Jpn. J. Appl. Phys.* 49, 07HF20.
- Kim, K., Kim, J.H., Park, H., Kim, Y.S., Park, K., Nam, H., Lee, S., Park, J.H., Park, R.W., Kim, I.S., Choi, K., Kim, S.Y., Park, K., Kwon, I.C., 2010. Tumor-homing multifunctional nanoparticles for cancer theragnosis: simultaneous diagnosis, drug delivery, and therapeutic monitoring. *J. Contr. Rel.* 146, 219–227.
- Lammers, T., Kiessling, F., Hennink, W.E., Storm, G., 2010. Nanotheranostics and image-guided drug delivery: current concepts and future directions. *Mol. Pharm.* 7, 1899–1912.
- Lammers, T., Aime, S., Hennink, W.E., Storm, G., Kiessling, F., 2011. Theranostic Nanomedicines. *Acc. Chem. Res.* 44, 1029–1038.
- Litzinger, D.C., Buiting, A.M.J., van Rooijen, N., Huang, L., 1994. Effect of liposome size on the circulation time and intraorgan distribution of amphipathic poly(ethylene glycol)-containing liposomes. *Biochim. Biophys. Acta* 1190, 99–107.
- MacKay, J.A., Li, Z., 2010. Theranostic agents that co-deliver therapeutic and imaging agents? *Adv. Drug Deliv. Rev.* 62, 1003–1004.
- Min, K.H., Kim, J.H., Bae, S.M., Shin, H., Kim, M.S., Park, S., Lee, H., Park, R.W., Kim, I.S., Kim, K., Kwon, I.C., Jeong, S.Y., Lee, D.S., 2010. Tumoral acidic pH-responsive MPEG-poly(beta-amino ester) polymeric micelles for cancer targeting therapy. *J. Contr. Rel.* 144, 259–266.
- Mohan, P., Rapoport, N., 2010. Doxorubicin as a molecular nanotheranostic agent: effect of doxorubicin encapsulation in micelles or nanoemulsions on the ultrasound-mediated intracellular delivery and nuclear trafficking. *Mol. Pharm.* 6, 1959–1973.
- Moon, G.D., Choi, S.W., Cai, X., Li, W., Cho, E.C., Jeong, U., Wang, L.V., Xia, Y., 2011. A new theranostic system based on gold nanocages and phase-change materials with unique features for photoacoustic imaging and controlled release. *J. Am. Chem. Soc.* 133, 4762–4765.
- Nagayasu, A., Uchiyama, K., Nishida, T., Yamagiwa, Y., Kawai, Y., Kiwada, H., 1996. Is control of distribution of liposomes between tumors and bone marrow possible? *Biochim. Biophys. Acta* 1278, 29–34.
- Nakamura, E., Makino, K., Okano, T., Yamamoto, T., Yokoyama, M., 2006. A polymeric micelle MRI contrast agent with changeable relaxivity. *J. Contr. Rel.* 114, 325–333.
- Nishihara, M., Imai, K., Yokoyama, M., 2009. Preparation of perfluorocarbon/fluoroalkyl polymer nanodroplets for cancer-targeted ultrasound contrast agents. *Chem. Lett.* 38, 556–557.

- Opanasopit, P., Yokoyama, M., Watanabe, M., Kawano, K., Maitani, Y., Okano, T., 2004. Block copolymer design for camptothecin incorporation into polymeric micelles for passive tumor targeting. *Pharm. Res.* 21, 2003–2010.
- Pan, D., Caruthers, S.D., Hu, G., Senpan, A., Scott, M.J., Gaffney, P.J., Wickline, S.A., Lanza, G.M., 2008. Ligand-directed nanobialys as theranostic agent for drug delivery and manganese-based magnetic resonance imaging of vascular targets. *J. Am. Chem. Soc.* 130, 9186–9187.
- Rapoport, N., Gao, Z., Kennedy, A., 2007. Multifunctional nanoparticles for combining ultrasonic tumor imaging and targeted chemotherapy. *J. Natl. Cancer Inst.* 99, 1095–1106.
- Rapoport, N.Y., Kennedy, A.M., Shea, J.E., Scaife, C.L., Nam, K.H., 2009a. Controlled and targeted tumor chemotherapy by ultrasound-activated nanoemulsions/microbubbles. *J. Contr. Rel.* 138, 268–276.
- Rapoport, N.Y., Nam, K.H., Gao, Z., Kennedy, A., 2009b. Application of ultrasound for targeted nanotherapy of malignant tumors. *Acoust. Phys.* 55, 594–601.
- Rapoport, N., Christensen, D.A., Kennedy, A.M., Nam, K.H., 2010a. Cavitation properties of block copolymer stabilized phase-shift nanoemulsions used as drug carriers. *Ultrasound Med. Biol.* 36, 419–429.
- Rapoport, N., Kennedy, A.M., Shea, J.E., Scaife, C.L., Nam, K.H., 2010b. Ultrasonic nanotherapy of pancreatic cancer: lessons from ultrasound imaging. *Mol. Pharm.* 7, 22–31.
- Rapoport, N., Nam, K.H., Gupta, R., Gao, Z., Mohan, P., Payne, A., Todd, N., Liu, X., Kim, T., Shea, J., Scaife, C., Parker, D.L., Jeong, E.K., Kennedy, A.M., 2011. Ultrasound-mediated tumor imaging and nanotherapy using drug loaded, block copolymer stabilized perfluorocarbon nanoemulsions. *J. Contr. Rel.* 153, 4–15.
- Sanson, C., Diou, O., Thévenot, J., Ibarboure, E., Soum, A., Brûlet, A., Miraux, S., Thi-audière, E., Tan, S., Brisson, A., Dupuis, V., Sandre, O., Lecommandoux, S., 2011. Doxorubicin loaded magnetic polymersomes: theranostic nanocarriers for MR imaging and magneto-chemotherapy. *ACS Nano* 5, 1122–1140.
- Schutt, E.G., Klein, D.H., Mattrey, R.M., Riess, J.G., 2003. Injectable microbubbles as contrast agents for diagnostic ultrasound imaging: the key role of perfluorochemicals. *Angew. Chem. Int. Ed. Engl.* 42, 3218–3235.
- Shiraishi, K., Kawano, K., Minowa, T., Maitani, Y., Yokoyama, M., 2009. Preparation and in vivo imaging of PEG-poly(L-lysine)-based polymeric micelle MRI contrast agents. *J. Contr. Rel.* 136, 14–20.
- Shiraishi, K., Kawano, K., Maitani, Y., Yokoyama, M., 2010. Synthesis of Poly(ethylene glycol)-b-poly(L-lysine) block copolymers having Gd-DOTA as MRI contrast agent and their polymeric micelle formation by polyion complexation. *J. Contr. Rel.* 148, 160–167.
- Solans, C., Izquierdo, P., Nolla, J., Azemar, N., Garcia-Celma, M.J., 2005. Nano-emulsions. *Curr. Opin. Colloid Interface Sci.* 10, 102–110.
- Tadros, T., Izuquiedo, P., Esquena, J., Solans, C., 2004. Formation and stability of nano-emulsions. *Adv. Colloid Interface Sci.* 108–109, 303–318.
- Tanigo, T., Takaoka, R., Tabata, Y., 2010. Sustained release of water-insoluble simvastatin from biodegradable hydrogel augments bone regeneration. *J. Contr. Rel.* 143, 201–206.
- Unger, E.C., Porter, T., Culp, W., Labell, R., Matsunaga, T., Zutshi, R., 2004. Therapeutic applications of lipid-coated microbubbles. *Adv. Drug Deliv. Rev.* 56, 1291–1314.
- Yamamoto, T., Yokoyama, M., Opanasopit, P., Hayama, A., Kawano, K., Maitani, Y., 2007. What are determining factors for stable drug incorporation into polymeric micelle carriers? Consideration on physical and chemical characters of the micelle inner core. *J. Contr. Rel.* 123, 11–18.
- Yokoyama, M., 2005. Polymeric micelles for the targeting of hydrophobic drugs. In: Kwon, G.S. (Ed.), *Drug and Pharmaceutical Sciences, Polymeric Drug Delivery Systems*, 148. Taylor & Francis, Boca Raton, pp. 533–575.
- Yokoyama, M., 2007. Polymeric micelles as nano-sized drug carrier systems. In: Domb, A.J., Tabata, Y., Kumar, M.N.V.R., Farber, S. (Eds.), *Nanoparticles for Pharmaceutical Applications*. American Scientific Publishers, Stevenson Ranch, pp. 63–72.
- Yokoyama, M., Opanasopit, P., Maitani, Y., Kawano, K., Okano, T., 2004. Polymer design and incorporation method for polymeric micelle carrier system containing water-insoluble anti-cancer agent camptothecin. *J. Drug Target.* 12, 373–384.
- Yuan, F., Dellian, M., Fukumura, D., Leunig, M., Berk, D.A., Torchilin, V.P., Jain, R.K., 1995. Vascular permeability in a human tumor xenograft: molecular size dependence and cutoff size. *Cancer Res.* 55, 3752–3756.
- Watanabe, M., Kawano, K., Yokoyama, M., Opanasopit, P., Okano, T., Maitani, Y., 2006. Preparation of camptothecin-loaded polymeric micelles and evaluation of their incorporation and circulation stability. *Int. J. Pharm.* 308, 183–189.

Suppression of Melanoma Growth and Metastasis by DNA Vaccination Using an Ultrasound-Responsive and Mannose-Modified Gene Carrier

Keita Un,^{†,‡} Shigeru Kawakami,^{*,†} Ryo Suzuki,[§] Kazuo Maruyama,[§] Fumiyoshi Yamashita,[†] and Mitsuru Hashida^{*,†,||}

[†]Department of Drug Delivery Research, Graduate School of Pharmaceutical Sciences, Kyoto University, 46-29 Yoshida-shimoadachi-cho, Sakyo-ku, Kyoto 606-8501, Japan

[‡]The Japan Society for the Promotion of Science (JSPS), Chiyoda-ku, Tokyo 102-8471, Japan

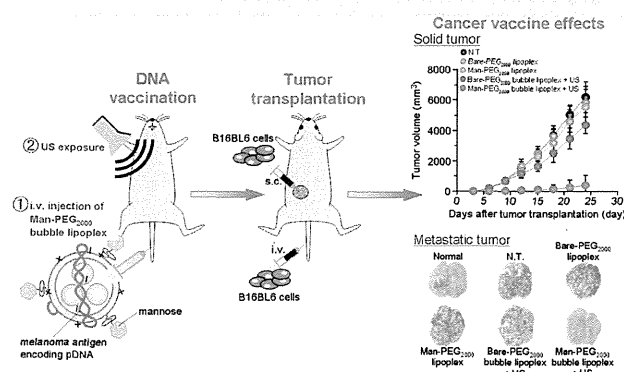
[§]Department of Biopharmaceutics, School of Pharmaceutical Sciences, Teikyo University, 1091-1 Suwarashi, Midori-ku, Sagami-hara, Kanagawa 252-5195, Japan

^{||}Institute for Integrated Cell-Material Sciences (iCeMS), Kyoto University, Yoshida-ushinomiya-cho, Sakyo-ku, Kyoto 606-8302, Japan

S Supporting Information

ABSTRACT: DNA vaccination has attracted much attention as a promising therapy for the prevention of metastasis and relapse of malignant tumors, especially highly metastatic tumors such as melanoma. However, it is difficult to achieve a potent cancer vaccine effect by DNA vaccination, since the number of dendritic cells, which are the major targeted cells of DNA vaccination, is very few. Here, we developed a DNA vaccination for metastatic and relapsed melanoma by ultrasound (US)-responsive and antigen presenting cell (APC)-selective gene carriers reported previously, named Man-PEG₂₀₀₀ bubble lipoplexes. Following immunization using US exposure and Man-PEG₂₀₀₀ bubble lipoplexes constructed with pUb-M, which expresses ubiquitinated melanoma-specific antigens (gp100 and TRP-2), the secretion of Th1 cytokines (IFN- γ and TNF- α) and the activities of cytotoxic T lymphocytes (CTLs) were specifically enhanced in the presence of B16BL6 melanoma antigens. Moreover, we succeeded in obtaining potent and sustained DNA vaccine effects against solid and metastatic tumor derived from B16BL6 melanoma specifically. The findings obtained from this study suggest that the gene transfection method using Man-PEG₂₀₀₀ bubble lipoplexes and US exposure could be suitable for DNA vaccination aimed at the prevention of metastatic and relapsed cancer.

KEYWORDS: mannose modification, bubble lipoplex, ultrasound, DNA vaccination, melanoma



INTRODUCTION

Melanoma is a neoplasm arising within epidermal melanocytes of the skin, and one of several cancers exhibiting the increasing incidence in recent years.¹ Early stage melanoma is curable, but melanoma metastasis and relapse occur frequently in the patients following treatments such as surgery, and the prognosis for patients with metastatic melanoma is poor.^{2,3} Although systemic therapy induces complete therapeutic responses in a minority of patients, metastatic melanoma is a devastating illness and treatment options are limited; therefore, there is a need for an effective therapy for metastatic melanoma.

Cancer vaccination has attracted much attention as a promising therapy for the prevention of tumor growth and metastasis, because it is based on an immune response provided by the cancer antigen, and consequently, its therapeutic effects are specific to the targeted cancer cells and the adverse effects followed by

cancer vaccination are low.^{4,5} In particular, it has been reported that DNA vaccination, which uses an exogenous gene encoding cancer antigen, can induce not only humoral immunity but also cellular immunity and, moreover, can induce cancer-specific CTLs with potent antitumor activities.^{6–9} In a variety of cancers, since melanoma is known to exhibit inherent immunogenicity and the identification of melanoma-specific antigen is proceeding, such as gp100, melanoma-antigen recognized by T cells-1 (MART-1) and tyrosinase-related protein (TRP),^{10–13} it is considered that DNA vaccination against melanoma is suitable for not only the

Received: October 29, 2010

Accepted: January 20, 2011

Revised: January 8, 2011

Published: January 20, 2011

prevention of metastasis and relapse but also the suppression of tumor growth.

To achieve potent therapeutic effects by DNA vaccination against cancer, it is essential to transfer the antigen-coding gene selectively and efficiently into APCs such as macrophages and dendritic cells, which play a pivotal role in the initiation, programming and regulation of cancer-specific immune responses.^{14,15} Our group has also developed mannose-modified liposome/plasmid DNA (pDNA) complexes (mannose-modified lipoplexes) for APC-selective gene transfer via mannose receptors expressing on APCs, and obtained APC-selective gene expression in the liver and spleen by mannose-modified lipoplexes.^{16,17} Moreover, our group also succeeded in obtaining DNA vaccine effects against cancer by intraperitoneal administration of mannose-modified lipoplexes constructed with tumor-specific antigen coding pDNA, such as ovalbumin (OVA) and melanoma-related antigens.^{18,19} However, the gene transfection efficiency into APCs was lower than that in other cells;²⁰ therefore, it could be difficult to induce a potent cancer vaccine effect for the prevention of metastasis and relapse by DNA vaccination using conventional lipofection methods.

It has been reported that cancer vaccine effects can be enhanced by physical stimulation-mediated gene transfer such as electroporation,^{21,22} hydrodynamic injection^{23,24} and sonoporation methods.²⁵ These transfection methods enable the delivery of a large amount of antigen-coding gene and antigen peptides into APCs, since exogenous materials are directly introduced into the cytoplasm without endocytosis in these methods.^{26–29} Recently, we have applied “sonoporation methods^{25,29–31}” using US exposure and microbubbles enclosing US imaging gas to enhance gene expression in APCs³² and developed a gene transfection method for DNA vaccination using US-responsive and mannose-modified gene carriers, Man-PEG₂₀₀₀ bubble lipoplexes.³³ This method enables APC-selective and -efficient gene expression, and moreover, effective vaccine effects against OVA-expressing cancer cells were obtained by applying this method to DNA vaccination using OVA-encoding pDNA.³³ However, the antigenicity of OVA is extremely high compared with other antigens,³⁴ and it is difficult to extrapolate the result obtained by DNA vaccination against OVA-expressing cells to actual cancer therapy, since OVA-expressing cells are transfectant constructed by gene transfer. Therefore, it is unclear if DNA vaccination by gene transfer using Man-PEG₂₀₀₀ bubble lipoplexes and US exposure is effective against cancer, i.e. melanoma, with metastatic properties.

In this study, we examined DNA vaccine effects against melanoma by transfection of pUb-M, coexpressing ubiquitinated gp100 and TRP-2, using Man-PEG₂₀₀₀ bubble lipoplexes and US exposure. First, we examined the level of gene expression in the splenic dendritic cells by gene transfer using Man-PEG₂₀₀₀ bubble lipoplexes constructed with pUb-M and US exposure. Second, we studied the characteristics of cytokine secretion and the induction of CTL activities against B16BL6 cell-derived melanoma by DNA vaccination using Man-PEG₂₀₀₀ bubble lipoplexes constructed with pUb-M and US exposure. Then, we investigated the cancer vaccine effects against solid and metastatic tumors derived from B16BL6 cells by DNA vaccination using Man-PEG₂₀₀₀ bubble lipoplexes and US exposure. Finally, we evaluated the duration of cancer vaccine effects against solid and metastatic melanoma after pUb-M transfection using Man-PEG₂₀₀₀ bubble lipoplexes and US exposure.

EXPERIMENTAL SECTION

Materials. 1,2-Stearoyl-3-trimethylammoniumpropane (DS-TAP), 1,2-distearoyl-*sn*-glycero-3-phosphocholine (DSPC) and 1,2-distearoyl-*sn*-glycero-3-phosphoethanolamine-*N*-[amino-(polyethylene glycol)-2000] (NH₂-PEG₂₀₀₀-DSPE) were purchased from Avanti Polar Lipids Inc. (Alabaster, AL, USA), Sigma Chemicals Inc. (St. Louis, MO, USA) and NOF Co. (Tokyo, Japan), respectively. Anti-CD11c monoclonal antibody (N418)-labeled magnetic beads were obtained from Miltenyi Biotec Inc. (Auburn, CA, USA). Fetal bovine serum (FBS) was purchased from Equitech-bio Inc. (Kerrville, TX, USA). RPMI-1640 and Dulbecco's modified Eagle's medium (DMEM) were purchased from Nissui Pharmaceutical Co., Ltd. (Tokyo, Japan). All other chemicals were of the highest purity available.

pDNA, Cell Lines and Mice. pUb-M containing murine melanoma glycoprotein-100_{25–33} (gp100) and tyrosinase-related protein-2_{181–188} (TRP-2) peptide epitopes was kindly provided by Prof. R. A. Reisfeld.³⁵ The B16BL6 melanoma cells, colon-26 adenocarcinoma cells and EL4 lymphoma cells were obtained from American Type Culture Collection (ATCC, Manassas, VA, USA). The B16BL6/Luc cells and colon-26/Luc cells, which are cell lines expressing firefly luciferase stably, were established as previously reported.^{36,37} The B16BL6 cells and EL4 cells were cultured in DMEM, and the colon-26 cells were cultured in RPMI-1640 at 37 °C in 5% CO₂. Both media were supplemented with 10% FBS, 100 IU/mL penicillin, 100 µg/mL streptomycin, and 2 mM L-glutamine. Female C57BL/6 mice (6 weeks old) and female Balb/c mice (6 weeks old) were purchased from the Shizuoka Agricultural Cooperative Association for Laboratory Animals (Shizuoka, Japan). All animal experiments were carried out in accordance with the Principles of Laboratory Animal Care as adopted and propagated by the U.S. National Institutes of Health and the Guidelines for Animal Experiments of Kyoto University.

Construction of Man-PEG₂₀₀₀ Bubble Lipoplexes. Man-PEG₂₀₀₀ bubble lipoplexes were constructed according to our previous report.³³ Briefly, DSTAP, DSPC and NH₂-PEG₂₀₀₀-DSPE or mannose-modified PEG₂₀₀₀-DSPE were mixed in chloroform at a molar ratio of 7:2:1 to produce the liposomes for bubble lipoplexes. The mixture for construction of liposomes was dried by evaporation and vacuum desiccated, and the resultant lipid film was resuspended in sterile 5% dextrose. After hydration for 30 min at 65 °C, the dispersion was sonicated for 10 min in a bath sonicator and for 3 min in a tip sonicator to produce liposomes. Then, the liposomes were sterilized by passage through a 0.45 µm filter (Nihon-Millipore, Tokyo, Japan). The lipoplexes were prepared by gently mixing equal volumes of pDNA and liposome solution at a charge ratio of 1.0:2.3 (–:+) . To enclose US imaging gas in lipoplexes, the prepared lipoplexes were pressured with perfluoropropane gas (Takachiho Chemical Industries Co., Ltd., Tokyo, Japan) and sonicated using a bath-type sonicator (AS ONE Co., Osaka, Japan) for 5 min. The particle sizes and zeta potentials of the liposomes/lipoplexes were determined by a Zetasizer Nano ZS instrument (Malvern Instrument, Ltd., Worcestershire, U.K.).

In Vivo Gene Transfection Method. Six week old C57BL/6 female mice were intravenously injected with 400 µL of bubble lipoplexes via the tail vein using a 26 gauge syringe needle at a dose of 50 µg of pDNA. At 5 min after the injection of the bubble lipoplexes, US (frequency, 1.045 MHz; duty, 50%; burst rate,